

# **DESIGN OF UPPER-BODY EXOSKELETON WITH MULTIFILAMENT MUSCLE ACTUATION AND BIOMIMETIC SUPPORT**

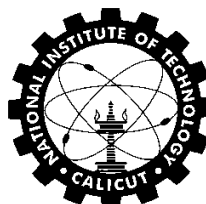
## **Project Report**

*Submitted in partial fulfillment of the requirements for the award of the degree of*  
**Bachelor of Technology**  
*in* **Mechanical Engineering**

**तमसो मा ज्योतिर्गमय**

*by*

<b>ARSHED AHMED</b>	<i>(Roll No.: B170325ME)</i>
<b>HYDER MUNDOLY</b>	<i>(Roll No.: B170895ME)</i>
<b>RAHUL K S</b>	<i>(Roll No.: B170104ME)</i>
<b>SOORYA NARAYANAN</b>	<i>(Roll No.: B170113ME)</i>



**तमसो मा ज्योतिर्गमय**

Department of Mechanical Engineering

NATIONAL INSTITUTE OF TECHNOLOGY CALICUT

MAY 2021

## CERTIFICATE

This is to certify that the report entitled "**DESIGN OF UPPER-BODY EXOSKELETON WITH MULTIFILAMENT MUSCLE ACTUATION AND BIOMIMETIC SUPPORT**" is a bonafide record of the **Project** done by **ARSHED AHAMMED T** (*Roll No.: B170325ME*), **HYDER MUNDOLY** (*Roll No.: B170895ME*), **RAHUL K S** (*Roll No.: B170104ME*) and **SOORYA NARAYANAN** (*Roll No.: B170113ME*), under my supervision, in partial fulfillment of the requirements for the award of the degree of **Bachelor of Technology** in **Mechanical Engineering** from **National Institute of Technology Calicut**, and this work has not been submitted elsewhere for the award of a degree.



**Dr. Gangadhara Kiran Kumar L**  
(Guide)  
Asst. Professor  
Dept. of Mechanical Engineering



**Dr. Sandip Rudha Budhe**  
(Co-guide)  
Asst. Professor  
Dept. of Mechanical Engineering

### **Professor & Head**

*Dept. of Mechanical Engineering*

Place : NIT Calicut  
Date : 30 MAY 2021

## **ACKNOWLEDGEMENT**

This project would not have been feasible without the kind support and assistance of many individuals and organizations. We want to thank every one of them from the bottom of our hearts. Dr. Gangadhara Kiran Kumar L, and Dr. Sandip Rudha Budhe, our guides, deserve special thanks for their guidance and regular supervision, as well as for providing crucial project information and support in completing the project. We would like to express our gratitude to the authors of the papers from which we were able to glean important material for our thesis. We'd also want to thank a variety of technical entities for contributing to our project by assisting us with their expertise.

## **ABSTRACT**

Exoskeletons are wearable devices placed on the user's body to augment, reinforce, or restore human performance. Factory workers who use exoskeletons have less back and shoulder pain and they can be more physically active both on the clock and off. Exoskeletons can transfer the weight of a user's arms from the shoulders, neck, and upper body to the body's core, reducing physical stresses. Pneumatic exoskeletons increase strength and provide stability through human-guided flexion/extension and locking mechanisms.

The main objective of the project is to develop a torso exoskeleton that facilitates load distribution and dynamic load compensation features. Providing an alternate load pathway to transfer the load from the shoulders to the pelvis, in addition to the human spine. Exo-Suit's limb actuator devices and sensors in the design will be based on study and analysis of human Musco-skeletal impact, measured during the person's interaction with the external environment.

Through this project, we try to find a faint balance between sufficient load-bearing for human augmentation and sufficient flexibility a "best of both worlds" of sorts. Moreover, we plan to design a load-bearing suit that comprises antagonistic actuators that emulate the structure of the human muscoskeleton. As a further note, we plan to add a microcontroller probably an FGPA Array, and its attributes to enable a control system that will help us monitor and survey the human requirements as well as the expected output. In short just as you would picture the human body in its inherent muscular form, we plan to add a second layer of muscle of McKibben form so that the extra layer of muscle bridges the gap between the human limit and superior strength.

## CONTENTS

<b>List of Abbreviations</b>	<b>viii</b>
<b>List of Symbols</b>	<b>ix</b>
<b>List of Figures</b>	<b>x</b>
<b>List of Tables</b>	<b>xiii</b>
<b>1 INTRODUCTION</b>	<b>1</b>
1.1 Introduction	1
1.2 Problem Definition	2
1.3 Exoskeleton Design	2
1.4 Outline of Report	3
<b>2 REVIEW OF LITERATURE</b>	<b>4</b>
2.1 Introduction	4
2.2 Design of Exoskeleton	5
2.2.1 Axes of Motions	5
2.2.2 Machine-Human Interactions	6
2.2.3 Hand Complex	7
2.2.4 Kinematics	8
2.2.5 Design of Artificial Muscles	9
2.2.6 Back Complex-Biological Aspects	10
2.2.6.1 The Backbone	10
2.2.6.2 Vertebrae	10
2.3 EMG Signal	11
2.4 Control Scheme	12
2.5 Gaps In Research And Objectives	13
2.6 Summary	13
<b>3 CONCEPTUAL DESIGN</b>	<b>15</b>
3.1 Introduction	15
3.2 Design Requirements	15
3.2.1 Shoulder Complex	15

3.2.2 Elbow Complex	16
3.2.3 Hand Complex	16
3.2.4 Back Complex	17
3.2.5 McKibben Fibre	17
<b>4 MATHEMATICAL MODEL</b>	<b>18</b>
4.1 Introduction	18
4.2 Force Calculation of Mckibben Muscle	18
4.2.1 Force Requirement for Each Biceps	19
4.2.2 Theoretical Calculation of Force Exerted by One Fibre of Mckibben Muscle	19
4.2.3 Force And Design Calculation for Back Muscle	25
<b>5 DETAILED MECHANICAL DESIGN</b>	<b>27</b>
5.1 Introduction	27
5.2 Mckibben Muscles	27
5.3 Back Complex	28
5.4 Shoulder Mechanism	29
5.5 Elbow Complex	30
5.6 Hand Complex	32
5.7 Exoskeleton	33
5.8 Kinematic Modeling of Arm	35
5.8.1 Drawing of Arm of Exoskeleton	37
5.8.2 Transformation Matrices	38
5.9 Dynamic Modeling of Exo-suit	39
5.9.1 Defining Exo-suit Hand in Matlab	40
5.9.2 Results	41
<b>6 SENSING AND CONTROL</b>	<b>43</b>
6.1 Introduction	43
6.2 Electromyogram	43
6.3 EMG Signal Acquisition	44
6.4 Valves and Compressor	46

<b>7 CONTROL</b>	<b>48</b>
7.1 Introduction	48
7.2 Control Logic	48
7.3 Pneumatic Control	49
7.4 PID Scheme	52
<b>8 RESULTS AND DISCUSSION</b>	<b>54</b>
8.1 Results	54
8.1.1 Derivation of Braid Angle Relation	54
8.1.2 Statistical Structural Analysis	55
8.1.2.1 Shoulder Complex	56
8.1.2.2 Elbow Complex	59
8.1.2.3 Back Complex	64
8.1.2.4 Exoskeleton	65
8.3 Kinematic and Dynamic Model	68
8.4 Control	68
<b>9 CONCLUSION AND SCOPE FOR FUTURE WORK</b>	<b>69</b>
9.1 Conclusion	69
9.2 Scope for Future Work	70
<b>REFERENCES</b>	<b>72</b>
<b>APPENDIX I: Properties of Materials Used</b>	<b>74</b>
<b>APPENDIX II: Error Calculation for Empirical Formulae to Obtain Braid Angle</b>	<b>75</b>
<b>APPENDIX III: Drawings of CAD Model</b>	<b>77</b>
<b>APPENDIX IV: Technical Details of Simulation Work</b>	<b>81</b>
<b>APPENDIX V: Code for Computer-Based Implementation</b>	<b>82</b>

## **LIST OF ABBREVIATIONS**

AC	Alternating Current
AFC	Active Force Control
AgCl	Silver Chloride
BE	Body Extender
CMRR	Common Mode Rejection Ratio
COR	Center Of Rotation
DC	Direct Current
DH	Denavit Hartenberg
DOF	Degree Of Freedom
EMG	Electromyography
FOS	Factor Of Safety
G-H	Glenohumeral
HMI	Machine Interface
LHS	Left Hand Side
MCP	Metacarpophalangeal
NHMI	Neural Hmi
PAM	Pneumatically Activated Muscle
PD	Proportional Differential Controller
PID	Proportional Integral Controller
RCM	Remote Center Mechanism
RHS	Right Hand Side
ROMS	Range Of Motion
SAA	Shoulder Abduction/Adduction
SC	Shoulder Complex
SEMG	Surface Electromyography
SFE	Shoulder Flexion/Extension
SR	Shoulder Internal/External Rotation
UB	Upper Body

## LIST OF SYMBOLS

$\alpha$	Braiding angle
$\alpha_f$	Final braiding angle
$\varepsilon$	Contraction ratio
$\varepsilon_c$	Circumferential strain
$l_0$	Initial Length of McKibben muscle
$l$	Final length of McKibben muscle
$t_b$	Thickness
$D_0$	Outer diameter
$E_b$	Elastic modulus
$F$	Force exerted by the McKibben muscle
$K$	Constant of proportionality between $P$ and $EMG_{value}$
$\Delta R$	Difference in radius
$R_0$	Initial outer radius
$R$	Final outer radius
$P_{app}$ or $P$	Applied pressure
$P^*$	Effective pressure
$P_{th}$	Threshold pressure

## LIST OF FIGURES

<b>No</b>	<b>Description</b>	<b>Page</b>
2.1	McKibben muscles	4
2.2	Multifilament Muscles	4
2.3	Myoelectric control System	4
2.4	Movable range of proposed ETS-MARSE.	5
2.5	Different Parts of ETS Marse	6
2.6	Mechanism of four-bar linkage	7
2.7	Shoulder design with double parallelogram	8
2.8	McKibben muscle	9
2.9	Spine structure	10
2.10	Electromyography	11
2.11	Block diagram for EMG signal acquisition	12
4.1	McKibben muscle braiding angle	18
4.2	FBD of back muscle	25
5.1	CAD of McKibben muscle	28
5.2	Back complex	28
5.3	Part-1 shoulder	29
5.4	Part-2 shoulder	29
5.5	Shoulder complex	30
5.6	Upper- limb	31
5.7	Elbow joint	31
5.8	Forearm-LHS	31
5.9	Forearm-RHS	31
5.10	Elbow complex	31
5.11	Finger complex	32
5.12	Hand complex	32
5.13	Muscles complex	33
5.14	Exoskeleton	33
5.15	CAD model of Exosuit	34

5.16	Reference axis	36
5.17	DH representation of one hand of our exosuit	36
5.18	CAD of hand	37
5.19	Details of exo-suit hand in Matlab	40
5.20	Diagram of exo-suit hand in Matlab	41
5.21	Output for static inverse dynamics	42
5.22	Output for inverse dynamics with external force	42
5.23	Output for forward dynamics	42
6.1	Basic flow circuit	44
6.2	EMG circuit	45
6.3	EMG gel electrodes placed on the subject	45
6.4	Equivalent magnetic circuit	46
7.1	Simulink block for proportional solenoid valve	50
7.2	Simulink block of exo-suit physical model	51
7.3	Simulink block for muscle model	51
7.4	Overall Simulink system for suit control	52
7.5	Schematic of a PID controller	53
8.1	Graphical relationship between twist angle and braiding angle	54
8.2	Graphical relationship between muscle length and braid angle	55
8.3	FOS distribution in Part 2-SC	56
8.4	Von mises stress distribution in part 2-SC	56
8.5	FOS distribution in part 1-SC (RHS)	57
8.6	Von mises stess distribution in Part 1-SC (RHS)	57
8.7	FOS distribution in Part 2-SC (LHS)	58
8.8	Von Mises stress distribution in Part 2-SC (LHS)	58
8.9	FOS distribution in Part 1-SC (LHS)	58
8.10	Von mises stress distribution in partn1-SC (LHS)	59
8.11	FOS distribution in forearm-RHS	59
8.12	Stress distribution in forearm-RHS	60
8.13	FOS distribution in elbow-joint RHS	60
8.14	Stress distribution in elbow joint RHS	60

8.15	FOS distribution in upper limb RHS	61
8.16	Stress distribution in upper limb RHS	61
8.17	FOS distribution in forearm LHS	61
8.18	Stress distribution in forearm LHS	62
8.19	FOS distribution in elbow joint LHS	62
8.20	Stress distribution in elbow joint LHS	62
8.21	FOS distribution in upper limb LHS	63
8.22	Stress distribution in upper limb LHS	63
8.23	FOS distribution in back complex	64
8.24	Stress distribution in back complex	64
8.25	Variation of FOS w.r.t Load	65
8.26	Variation in stress w.r.t Load	65
8.27	Stress-Strain curve of the suit	66
8.28	FOS distribution in exoskeleton	66
8.29	Stress distribution in exoskeleton	67

## LIST OF TABLES

No	Description	Page
1.1	Mean segment length of healthy subject	4
4.1	$P_{th}$ VS wall thickness of bladder	4
5.1	Properties of back	4
5.2	Properties of Part 1 and Part 2	5
5.3	Properties of components in elbow complex	6
5.4	Properties of hand complex	8
5.5	Properties of exoskeleton	8
5.6	DH parameter table for kinematic analysis	10
5.7	DH parameter table for dynamic analysis	12
6.1	Pressure vs wall thickness for range of pressure	14
8.1	Simulation results: SC LHS	14
8.2	Simulation results SC-RHS	15
8.3	Strength analysis in elbow complex	17
8.4	Simulation results in exoskeleton	19

# **CHAPTER 1**

## **INTRODUCTION**

### **1.1 INTRODUCTION**

Exoskeletons are wearable devices placed on the user's body to augment, reinforce, or restore human performance. Factory workers who use exoskeletons have less back and shoulder pain and they can be more physically active both on the clock and off. Exoskeletons can be used instead of industrial robots and eliminate the need for completely automated solutions. Exoskeletons can also help aging workers continue to perform labor-intensive tasks. The largest benefit is to decrease worker injuries and reduce healthcare and disability costs. Employee turnover is also reduced. Carrying a heavy backpack can increase the risk of musculoskeletal injuries. Injuries on the upper body are mainly caused by accumulated stress on the spine and lumbar muscles required to support the additional loads on the shoulders and to maintain postural stability while walking.

### **1.2 PROBLEM DEFINITION**

Each of the muscular motions is measured for its correlated moment on the joints so that a similar smooth response from the Exo-Suit can be obtained. As of now mostly PAMs are used for actuation in exosuits which although provides much sturdiness and contraction force but compromises on the most degree of freedoms (dofs). As a means to solve this and improve the flexibility of the suit and user, we plan to use thin McKibben muscles specifically multifilament muscles. This type of muscle actuator has been experimented on in robots that try to replicate human nature but have not been fully implemented in the forte of exosuits. McKibben muscles of this kind have a compromising issue: namely, they are less strong or there is a significant reduction in the load-bearing capabilities. However a relation is established here; that as we decrease the diameter of the said muscles and make it more "thinner", the contraction ratio is reduced by comprising on the contraction force.

### 1.3 EXOSKELETON DESIGN

Several exoskeletons are already developed such as MIT MANUS made by the students of MIT University, ETS-MARSE, CADEN-7, IntelliArm, ARMin made by ETH Zurich, etc. Starting from the initial stages of making the exoskeleton many research papers available about the existing exoskeleton was read. Every robot team has taken a healthy subject as a model for the dimensions. Hence it can be deduced that obtaining the dimensions from the human model considered and making the mechanism compatible for others with size ratio will aid in the manufacturing process.

Using finger and the palm dimensions and all ranges of motions involved from adequate literature study, the various kinematic and dynamic analytical studies were undertaken, and the datasets are documented below. Using the data obtained from the study conducted by Plagenhof et al. [1], measurements taken are shown in Table 1.1

Table 1.1: Mean segment lengths of healthy subject [1]

Segment	Length/mm (Man)
Hand	106
Forearm	438
Upper hand	402
Whole trunk	569
Shoulder to Shoulder	640

The necessities for developing an effectual and precise exoskeleton are:

- Adaptable: It can be fabricated for people of all age groups, as each part involved in the exoskeleton can be fabricated according to the corresponding dimensions of the subject involved.
- Lightweight: The overall weight of the exoskeleton should be such that it enables easy and burden-free handling by the subject involved. This is done by fabricating the mechanism using lightweight yet strong and rigid materials.
- Large ranges of motion: It helps to enable the subject in achieving all-natural ranges of motions involved in the human movement by appropriate positioning of the actuators.

- Alignments of natural axes: It is essential to align the axes of the exoskeleton with that of the subject involved, for proper movement of all the joints, while maintaining the natural gait and ranges of motion involved at the same.

## 1.4 OUTLINE OF REPORT

The basic idea behind this project is to design a suit that will employ the advantages of Multifilament McKibben muscles to provide power augmenting capabilities without letting the flexibility suffer. The design proposed although theoretical shows promise. As a part of this continued project work, first, we see in this report the literature that was used for the study and extrapolation into our specific work. Important suits like BE and AXO Suit that have made significant contributions to the field of exo-suits are studied and checked to see if the structural design, as well as control mechanisms, can be picked up and used for our project. Moving on, the conceptual design of our system is modeled in CAD as well as the single muscle strand that is the power behind the suit. Further, the input mechanisms i.e, the EMG module being implemented is studied and the results that it produces are studied to establish further benchmarks. Control logic that will monitor and make the character got the suit is reviewed and awaits further study and modeling. Necessary calculations based on the constants chosen earlier were completed and this establishes the base of our further work. The report then winds up with discussing the results and then states the future work that has to be done to furnish the project.

## CHAPTER 2

### LITERATURE REVIEW

#### 2.1 INTRODUCTION

These are smaller McKibben muscles that work on pneumatic actuation.



Figure 2.1 McKibben muscles

They are analogous to human muscle strands and are bundled together to form a "multifilament muscle".

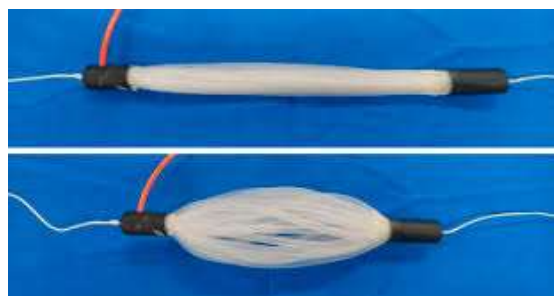


Figure 2.2 Multifilament Muscles

A Myoelectric Control System can be used for actuating the limbs. This system utilizes a microcontroller that takes input from electromyography signals from the EMG sensors. Surface EMG sensors are used due to their simplicity and non-invasive technique. Power sent to an actuator is proportional to the amplitude of the normalized EMG signal from a muscle.

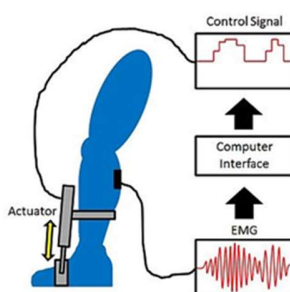


Figure 2.3 Myoelectric Control System

## 2.2 DESIGN OF EXOSKELETON

Existing robots don't seem to be nonetheless ready to restore bodily quality or operate. This can be because of limitations within the space of correct hardware style which of management algorithms. A number of the notable hardware limitations within the existing skeleton systems embody restricted degrees of freedom and vary of motion as compared with human higher extremities [2].

### 2.2.1 Axes of Motions

- The exoskeleton contains the subsequent 3 parts: shoulder motion support, elbow and forearm motion support, and carpus motion support.

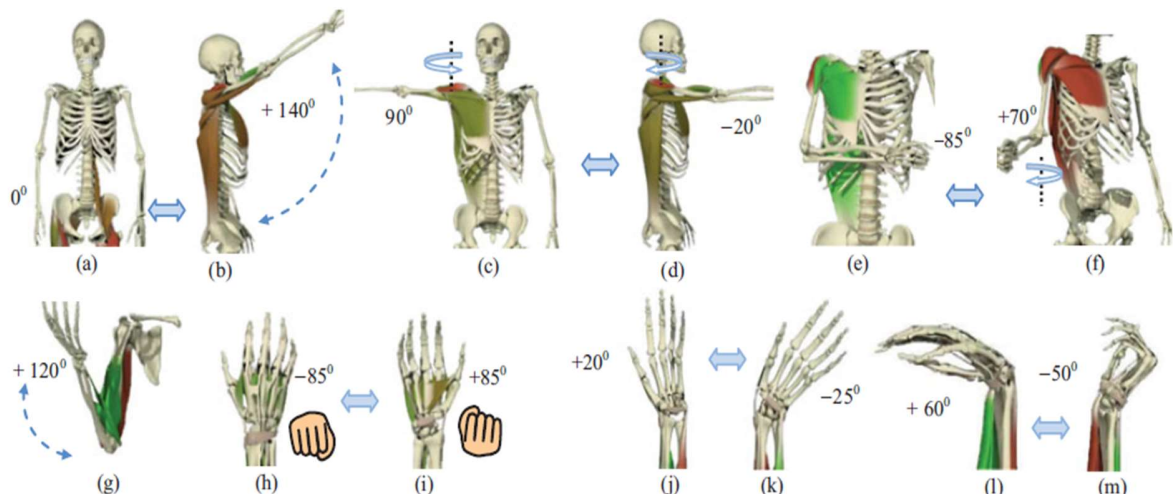


*Figure 2.4 (Colour online) Movable range of proposed ETS-MARSE. (a) Initial (zero) position; (b) shoulder joint: vertical flexion; (c) shoulder joint: horizontal extension; (d) shoulder joint: horizontal flexion; (e) shoulder joint: internal rotation. (Source: <https://www.cambridge.org/core>)*

- Shoulder motion, as an example, composed of glenohumeral (G-H), acromioclavicular, and sternoclavicular articulations may be delineated mostly by the G-H joint for a range of arm activities involving up to 90° of arm elevation.
- A ball and socket joint composed of 3 orthogonal axes decussate at the middle of the humeral head, though the true center of rotation is thought to vary with arm orientation.
- The elbow may be delineated as a single-axis hinge joint wherever the hinge rests at an associate degree angle with relevancy to each higher and lower arm segment underneath full-arm extension.

- The articulatio plana may be modeled as 2 orthogonal axes with a hard and fast offset between them. The proximal and distal axes of the articulatio plana correspond to articulatio plana flexion-extension and articulatio plana radial-arm bone deviation, severally.

Articulation of the exoskeleton is achieved about seven single-axis revolute joints [3]:

- 1) Shoulder abduction-adduction
- 2) Shoulder flexion-extension
- 3) Shoulder internal-external rotation,
- 4) Elbow flexion-extension
- 5) Forearm pronation-supination
- 6) Wrist flexion-extension
- 7) Wrist radial-ulnar deviation.

### 2.2.2 Machine-Human Interactions

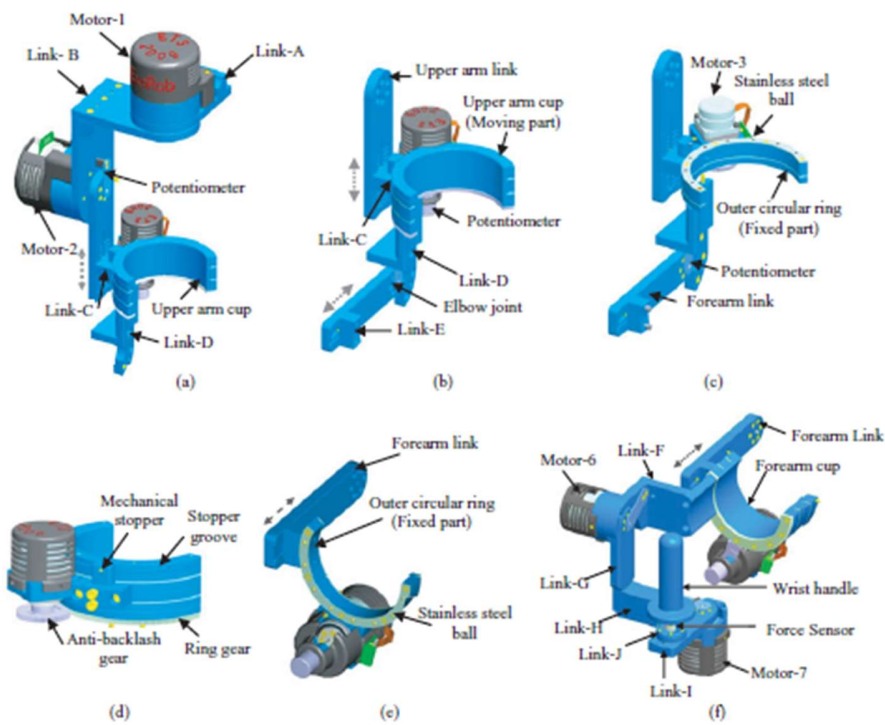


*Figure 2.5 (a) Shoulder motion support part; (b) Internal/external rotation support part (when elbow motor is unplugged from elbow joint); (c) showing custom-made, open-type bearing when upper arm cup is not assembled; (d) actuation mechanism for the shoulder. (Source: <https://www.cambridge.org/core>)*

- Proximal placement of motors and distal placement of cable-pulley reductions were incorporated into the look, resulting in low inertia, high stiffness links, and backdrivable transmissions with zero backlash.
- The human-machine interface (HMI) of the operator/ skeleton is meant to come up with the natural operation of the device. The neural HMI (HMI) is ready at the contractor level of the human physiological hierarchy, exploitation processed sEMG signals together of the first command signals to the system
- The largest needed ROM square measure found in elbow flexion-extension and forearm pronosupination, every at 150°, whereas the necessity from shoulder flexion-extension, the joint having the biggest physiological storage, remains less at 110° [3].
- Alternatively, body interferences may be removed through substitution of the complete bearing with a partial bearing wherever the bearing track is basifixated to the proximal systema skeletale link.
- Given a configuration that meets this criterion, further codependent issues like link excursion, energy consumption, and collision rejection with the body ought to be taken into consideration.

### 2.2.3 Hand Complex

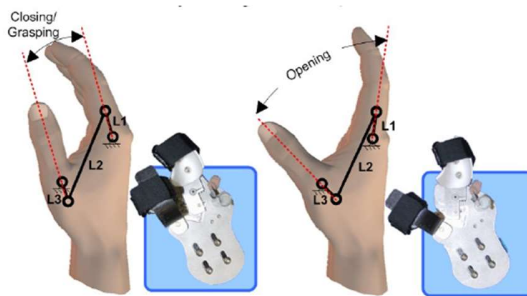


*Figure 2.6: The mechanism of a four-bar linkage used to generate hand opening and closing motion.*

(Source: <https://ieeexplore.ieee.org/>)

- The appliance of the rehabilitation robotic arm, the sophisticated and cumbersome hand frame system would be connected on the tip of the automaton arm, and therefore it might probably scale back the driven ability and motility of the total automaton arm owing to its weight and inertia.

- Experiments indicate that within the hand rehab coaching, the hand gap and shutting coaching plays a key role, followed by the coaching of different tiny finger joints.
- The principle of four-bar linkage to get the hand grasping combined motion with the only motor-driven. The motor can rotate the link L1 to open MCP joints of all four fingers; link L3 can push the thumb away synchronously. The combined motion between L1 and L3 can simulate a hand gap and shutting motion [4].

#### 2.2.4 Kinematics

The FB-AXO [5] system contains twenty-seven degrees of freedom, of that seventeen area unit passive and ten active. Highest priority lower body motions: Lifting/dropping while not grasping and going to the aspect overhead/opposite shoulder. The approach is adopted for the full-body AXO-SUIT frame to accommodate the massive manual dexterity of the human arm, the UB-AXO contains a total of fifteen degrees of freedom, 3 at the spine module, 5 at every shoulder module, and one at every elbow module. The UB-AXO includes 2 novel styles, namely, a bio-mimetic spine module and a shoulder module designed with double parallelograms. The shoulder abduction/adduction (SAA) and flexion/extension (SFE) joints area unit hopped-up, whereas the shoulder internal/external rotation (SR) joint is passively supported by a double quadrilateral linkage.

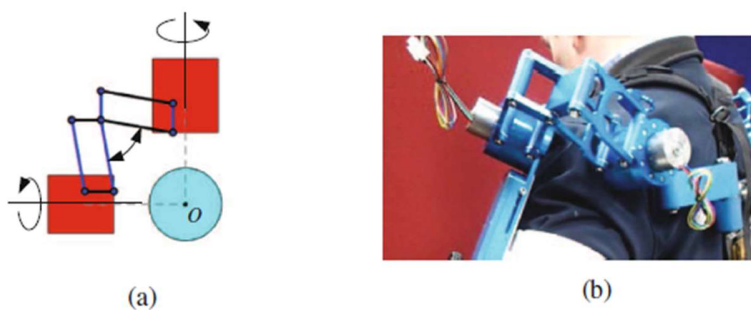


*Figure 2.7: The novel shoulder joint designed with double parallelograms, (a) kinematic principle, where three rotations are noted, (b) construction of shoulder joint in the upper-body exoskeleton  
(Source: <https://www.researchgate.net>)*

## 2.2.5 DESIGN OF ARTIFICIAL MUSCLES

- The McKibben muscle [6] is taken into account as an excellent mechanism for wearable management suits and contractile organ robots since its compliance characteristics and withdrawal properties are unit comparative to those of human muscles.
- McKibben muscles cannot be mounted thickly in contractile organ robots and it's difficult to induce a repetitive drive part for their rise to its human muscles.
- The advantage of the gas muscles being light-weight has not but been adequately used since of such an expansive and overwhelming body covering. This mechanism is in addition a lot of lightweight and compact than different routine gas muscles.
- The elastic tube extends at intervals the spiral course at a lower place connected weight and this ends up in a withdrawal force/displacement at intervals the important course by dynamical the passementerie purpose.
- The hardness of the interior tube impacts the characteristics of the lean McKibben muscle. Once the amount of outer fibers is expansive, withdrawal constraints increments; be that because it might, the withdrawal proportion is remittent.
- On the off probability that the amount of external strands is not adequate, the lean McKibben muscles effortlessly burst, and also the range of external filaments should be a lot of than 24.

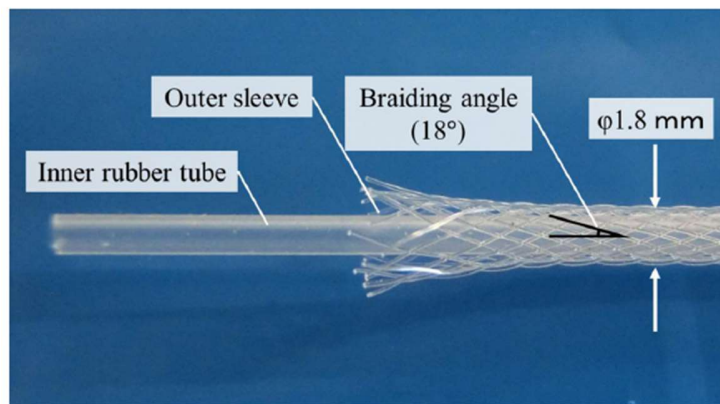


Figure 2.8: Thin McKibben muscle comprising an inner tube and outer sleeve. The braiding angle is 18°

(Source: <https://www.journals.elsevier.com/sensors-and-actuators-a-physical>)

## 2.2.6 BACK COMPLEX-Biological Aspects

### 2.2.6.1 The backbone

The spine (Fig. 2.9) is a portion of the polar skeleton and goes from the bottom of the brainpan to the pelvis. In people, it's fabricated from articulating vertebrae, whose work is to produce quality and flexibility to the vertebral column.

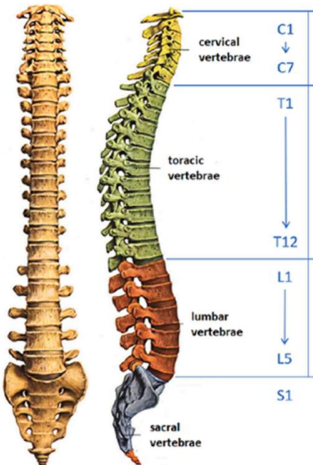


Figure 2.9: Spine structure for the kinematics analysis (Source: <https://http://www.elsevier.com/locate/ergon>)

The vertebrae area unit named agreeing to the venue of the spine to that they need a place; unremarkably, there is seven cervical (C1–C7), twelve thoracics (T1-T12), five body part (L1-L5), five sacral (S1–S5), and three to five bone vertebrae [7].

### 2.2.6.2 Vertebrae

A typical vertebra is composed of cancellous bone covered by a thin coating of cortical bone. This part of the vertebra has the aim of supporting the head and the trunk weight. The vertebral arch, instead, is posterior. It is formed by a pair of pedicles, laminae, and supports seven processes, four articular, two transverse, and one spinous. The articular processes are characterized by the presence of facet joints covered with cartilage. The transverse processes project from either side and constitute the attachment of muscles and ligaments, in particular the intertransverse ligaments.

## 2.3 EMG SIGNAL

An electromyography (EMG) sensor is used for obtaining the input signal for our exosuit. A potential difference is created in the neurons of our muscle fibers as it contracts and expands, the EMG sensor continuously measures this potential difference across our muscle. Surface EMG electrode is used instead of needle electrode due to its non-invasive technique and simple setup. The AgCl gel electrodes are mostly preferred for obtaining the accurate value of EMG. The AgCl layer in the electrode allows current from the muscle to pass more freely across the junction between the electrolyte and the electrode. Thus, only a feeble electrical noise is introduced in the measurement.

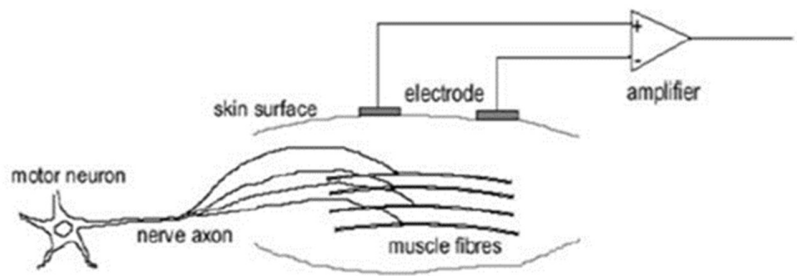


*Fig 2.10 Electromyography (source: www.ijert.com)*

CMRR, Common Mode Rejection Ratio is the measure of the ability of a differential circuit to suppress the signals, which are common in both the inputs. The CMRR should be as high as possible because the elimination of interfering signals plays a major role in the quality of the acquiring signal. EMG signal in the range of 50-500Hz is required for detection of muscle activity, so the band pass filter can be set accordingly. [8]

$$CMRR = \log \frac{V_{OUT}}{V_{IN}} dB \quad (1)$$

A differential amplifier with a high CMRR ratio can be used as the first stage of processing, its advantage is that the elements which are common in both the signal inputs are subtracted by this differential amplifier. [9] The AD620 performs well as a preamplifier as it has a low input voltage noise, and high CMRR (120-130). High pass filter of 20Hz and low pass filter of 650Hz (most of the EMG falls in this frequency range). It is really important to

obtain the EMG data in the low-frequency region as the majority of information lies in this region.

The best method for converting the filtered EMG signal into DC signals is by taking the Root Mean Square of a window of data points. An Arduino Uno microcontroller can be used to convert AC to DC using the root mean square method.

$$RMS = \sqrt{\frac{1}{n} \sum_n x^2(t)} \quad (2)$$

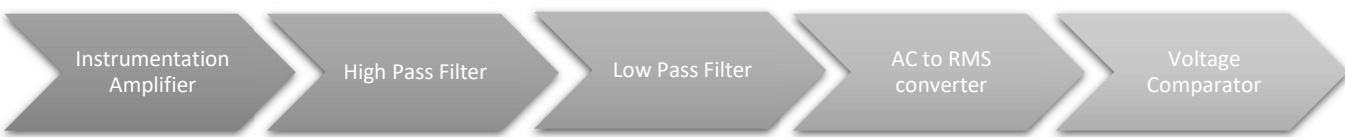


*Figure 2.11 Block Diagram of the proposed system for EMG signal acquisition and processing*

## 2.4 CONTROL SCHEME

- The paper [10] talks about the design of a PID, PD, and P control for a robotic arm that is actuated by a PMDC motor.
- Mathematical modeling of the system and its dynamics are studied in this paper along with the necessary transfer functions that come into play once the system is modeled in software.
- The paper however describes the PID controller as a sufficiently strong model in controlling the arm of the lot, although higher precision would result in complexity.
- This paper [11] deals with the modeling of a simple AFC system for a two-link rigid arm. It talks about the involvement and importance of components like Coriolis and gravity along with the mass of the robot arm as important factors in torque control.
- AFC or active force control is a scheme that gives a relief control system that is otherwise perturbed due to noises.
- A comparison is made between the AFC scheme and PID control loop usually used and AFC was found to better eliminate disturbance although it requires a more complex structuring.

- Discusses [12] “extenders”, which are suits worn to augment human strength, and how the modeling might be carried out.
- Augmentation capabilities are studied based on continuous inputs from two systems, namely: human-suit and suit-environment.
- Closed-loop stability is included so that proper control of the suit is achieved.
- The suit is judged based on how well it fares against prescribed conditions and to what extent the suit can amplify the user's human limitations.

## **2.5 GAPS IN RESEARCH AND OBJECTIVES**

Based on the literature study it is clear that in the existing exoskeletons, the axes of girdle movements are not aligned with that of human joints, the exoskeleton as a whole is bulky and non-ergonomic, not much importance was given to finger part and so on. Therefore, the objective of the project is to develop an exoskeleton that is lightweight, adaptable, ergonomic, which has a large range of motion and force control. This exoskeleton also ensures the alignment of rotational axes consistent with anatomic considerations for proper movement of all the joints, while maintaining the natural gait and ranges of motion involved at the same. It also ensures limiting the creation of interface forces at the distal point.

- Design of an upper-body exo-suit that gives a power augmentation to the user.
- Design an exoskeletal suit that gives a power augmentation of  $2x \{(250*2)\}$  for each arm}
- Employ Multifilament McKibben muscles with pneumatic actuation.
- Obtain a sufficient balance between force and flexibility.
- Use EMG sensors for obtaining input from the wearer.
- Design a control law for the control of artificial muscles during working and give the feel of reduced effort to the wearer.

## **2.6 SUMMARY**

- Multifilament muscles triumph over ordinary McKibben muscles when contraction ratio and actuation methods are considered.
- Thicker bundles do not proportionally increase contraction force due to dead space.
- Multifilament muscles are a better choice for implementing muscles redundancy in robots

- Formulations have been made without considering hysteresis and other material factors-So Schutle's formula stands valid.
- The basic strand build contains an inner elastic tube, outer stiffer tube, covering mesh, clamps, and actuator.
- EMG signals have been employed in most designs although they produce significant noise.
- Proper filtering of signals should be done to avoid unwanted disturbances in the control.
- A PID force control implemented for every muscle used is a reliable control method although adding an AFC scheme with Fuzzy Logic might improve precision by about  $10^{-2}$ .

## CHAPTER 3

### CONCEPTUAL DESIGN

#### 3.1 INTRODUCTION

The main aims of this project are to

- Identify the major muscles involved in pushing and pulling, when a load is carried with a human arm.
- Calculate and simulate force supplied by the individual and total bundle for each muscle section.
- Conduct FEM analysis to understand load-bearing characteristics.
- Conduct an EMG test to understand and establish reference signals for further work.
- Design a control loop that works on the continuous input from EMG and reference signals established.
- Simulate the working of the suit under different conditions and develop a compiled model.

#### 3.2 DESIGN REQUIREMENTS

The upper-body exoskeleton design can be discussed under the four complexes:

1. Shoulder Complex
2. Elbow Mechanism
3. Hand Complex
4. Back Complex
5. McKibben Fiber

Each part has its components, motions, and all these components play an important role in the pneumatic actuation of the exoskeleton.

##### 3.2.1 Shoulder Complex

- The first point considered while designing the shoulder complex was the collision risks involved with them while human body interactions.
- There must be a set of three orthogonal axes of rotation in the shoulder mechanism, for motions such as internal-external rotation, abduction-adduction motion, and flexion-extension.
- Due to the presence of three orthogonal axes and the movements associated with them, the SC can be bulky and adds weight to the exoskeleton. Weight or

Bulkiness is an important factor that was considered while designing all components. Hence simplicity in design is given more priority.

- From the structural analysis point of view, the SC complex will experience a great amount of tension and bending moment when weight is carried by the exoskeleton. Also, the discontinuity in the components is reduced to a minimum possible to reduce stress-concentration.

### 3.2.2 Elbow Complex

- While designing the forearm part of the exoskeleton the antagonistic nature in the movement of the left and right arm was considered. The required range of motion, weight/bulkiness of the components, and forearm are one of the parts in the exoskeleton which come in direct contact with the load. All these factors were considered while designing the forearm components.
- The part that supports the upper limb of the hand is a relaxed component, the bending moment due to the load is balanced by McKibben muscle hence the component was made lightweight to avoid wastage of material. Also, the elbow flexion-extension motion was considered while designing the components. The discontinuities such as holes in this part will have more impact since a thin component is being modeled.
- While designing the part that acts as the elbow joint that connects the upper-limb part to the forearm part following factors was considered
  - That part has to make both the forearm pronation-supination motion and elbow flexion-extension possible.
  - Being a small component where both the bending moment from load and support from biceps McKibben muscle acts, the part was designed with fewer discontinuities and stronger material.

### 3.2.3 Hand Complex

- The hand exoskeleton to be developed needed the alignment of the exoskeleton with each of the joints of the finger i.e. MCP, PIP, and DIP.
- This component comes in direct contact with the load also plays an important role in grasping the weight.

- Since activation of human muscles plays an important role in the sensory circuit, this component is just designed as mechanical support for the human hand while carrying the load. Since the hand complex involves many small parts, load-displacement to this part is minimized. Hence structural analysis of this component is not considered while designing.
- Also, a structure with much flexibility can accompany many motions in the finger system. Hence small components with more DOFs were designed.

### **3.2.4 Back Complex**

- The back complex has the most reaction force and it is to be designed to carry the entire load applied to the exoskeleton also the weight of all the components in the exoskeleton.
- The back complex has to be firm at the time a little flexible to effectively carry the weight and factors like human body interaction, comfort has to be considered.
- Since the back complex is going to be the part all load is going to be applied, the part is at great risk of failure hence a scissor mechanism that can effectively displace the load is considered. This mechanism also adds a little flexibility to the complex.

### **3.2.5 McKibben Fibre**

Factors considered while designing

- Fiber diameter
- Tube internal, external diameters
- Length of the fiber
- Braid angle: Since in CAD software twist angle was the parameter input we can give, a relationship was developed connecting braid angle to twist angle and length of the fiber.

## CHAPTER 4

### MATHEMATICAL MODEL

#### 4.1 INTRODUCTION

For controlling McKibben muscle according to the hand movement it is necessary to give force which makes a similar kind of motion as our hand. For this, we need to control muscle force concerning input that we give to the McKibben which is pressure and pressure can be controlled by a valve that allows the passage of air to McKibben muscle. To get the value of pressure that we should give to get a particular force we had to establish a relationship between pressure and force of McKibben muscle. The basic formula available for the force exerted by McKibben was Shuttle's formula, Along with this formula we need to consider the dimensional change that would happen to the muscle while contracting.

#### 4.2 FORCE CALCULATIONS OF MCKIBBEN MUSCLE

Dimensions of McKibben muscle:

Braiding angle =  $18^0$

Length of McKibben muscle = 0.2m

Outer diameter ( $D_0$ ) = 6mm

Outer sleeve diameter = 0.4mm

For inner tube:

Outer diameter = 4.34mm

Inner diameter = 3mm

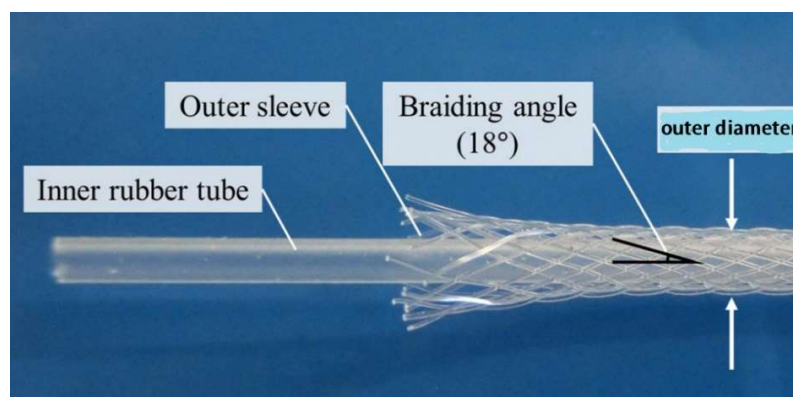


Figure 4.1 McKibben muscle

#### 4.2.1 Force requirement from each McKibben muscle for biceps

We intend to generate a force by the exoskeleton which is 2 times the force that our hand is applying. Generally, a normal human hand can lift a maximum of 25kg with one hand

The maximum force exerted by one human hand from the above lifting criteria;

$$F_{max} = 25 * 10 = 250N \quad (3)$$

Therefore the force required by the bundle of McKibben muscle on one hand;

$$F_{total} = 250 * 2 = 500N \quad (4)$$

Number of Muscles in a bundle of muscle on one hand = 16

The average force required by one McKibben muscle;

$$F_{fiber} = \frac{500N}{16} = 31.25N \quad (5)$$

The equation- (5) is based on assumption. In reality, the force exerted by a bundle of McKibben muscle will be less than the sum of the forces exerted by individual fibers due to many losses of nonrigidity of McKibben muscle and the unfilled gap between individual muscles.

#### 4.2.2 Theoretical calculation of force exerted by one fiber of McKibben muscle

The available formula for force calculation is Schulte's formula

$$F(P, \varepsilon) = \pi R_0^2 P \cdot (a(1 - \varepsilon)^2 - b) \quad (6)$$

$$a = \frac{3}{\tan^2 \alpha} \quad b = \frac{1}{\sin^2 \alpha} \quad (7)$$

$$\alpha = 18^\circ \quad (8)$$

$$F(P, \varepsilon) = \pi R_0^2 P \cdot \left( \frac{3}{\tan^2 \alpha} \times (1 - \varepsilon)^2 - \frac{1}{\sin^2 \alpha} \right) \quad (9)$$

$$F(p, \varepsilon) = \frac{\pi R_0^2 P^x}{\sin^2 \alpha} ((1 - \varepsilon^2) \cos^2 \alpha - 1) \quad (10)$$

$$P^* = P_{app} - P_{initial} \quad (11)$$

$$R_0 = \text{outer radius} \quad (12)$$

$$\varepsilon = \text{contraction ratio} = \frac{L_0 - L}{L_0} \quad (13)$$

We have the equation for maximum contraction ratio as

$$\varepsilon_{max} = 1 - \sqrt{\frac{b}{a}} = 0.3929 \quad (14)$$

From the research papers, maximum pressure that can be applied to a McKibben muscle fiber = 0.7 MPa

So McKibben muscle should give a contraction ratio of 0.3929 at the maximum pressure to avoid any failure

Assuming McKibben muscle as a pressurized rubber hollow cylinder having thickness  $t_b$ , Elastic modulus  $E_b$

Then the circumferential strain in the whole unit ie bladder and braid is given by

$$\varepsilon_c = \frac{\Delta r}{r_0} = \frac{P \cdot r_0}{E_b t_b} \quad (15)$$

Where  $\Delta r = r - r_0$

$r_0$ = unpressurized diameter

$r$  = pressurized diameter

$t_b$ = wall thickness

$P^*$  Is the threshold pressure, it is the pressure at which the bladder makes the first contact with the braid, only after that the above formula can be applied. For Shulte's formula to satisfy force relation for McKibben, the bladder should make contact with the braid.

$$P^* = P - P_{Th} \quad (16)$$

$P_{th}$  data for different thickness rubber hollow cylinders

Table 4.1  $P_{Th}$  VS Wall thickness of bladder:

X: Wall thickness (mm)	0.28	0.56	1
Y: $P_{th}$ (bar)	0.08	0.21	1.89

By linear regression;

$$y = a + bx \quad (17)$$

Where

$$a = \frac{\sum y \sum x^2 - \sum x \sum xy}{\sum x^2 - (\sum x)^2} = -0.321 \quad (18)$$

$$b = \frac{n \sum xy - \sum x \sum y}{n \sum x^2 - (\sum x)^2} = 2.630 \quad (19)$$

From (1)

$$y = -0.321 + 2.63x \quad (20)$$

Putting the desired value of thickness for x and y as 0.67 and 0.1441 MPa respectively

Now, taking the McKibben muscle as a hollow cylinder rubber, the inner radius of the braid and bladder will be the same if the bladder touches the braid.

$$\varepsilon_c = \frac{(P - P_{th})}{E_b t_b} \quad (21)$$

$\varepsilon_c$  Can be true for braid also if  $P > P_{th}$

$$\frac{\Delta R}{R_0} = \frac{(P - P_{th})R_0}{E_b t_b} \quad (22)$$

For braid and bladder;

$$\Delta R = \frac{R_0^2(P - P_{th})}{E_b t_b} \quad (23)$$

$\Delta R$  Is the change in radius for the inner part which is that of the outer part if the change in the thickness is neglected.

$$\frac{l}{l_0} = \frac{\cos \alpha_f}{\cos \alpha}, \quad \left( \frac{R}{R_0} \right)_{braid \ outer} = \frac{\sin \alpha_f}{\sin \alpha} \quad (24)$$

Where  $\alpha_f$  is the final braid angle after contraction

$$\left(\frac{l}{l_0} \cos \alpha\right)^2 + \left(\frac{R}{R_0} \sin \alpha\right)^2 = 1 \quad (25)$$

$$\Delta R \Rightarrow \left(\left(\frac{4.34}{2}\right) \times 10^{-3}\right)^2 \frac{(P - P_{th})}{E_b t_b} \quad (26)$$

For 0.7MPa;

$$\varepsilon = 0.3926 = \frac{L_0 - L}{L_0} \Rightarrow \frac{L}{L_0} = 0.6074 \quad (27)$$

$$\left(\left(\frac{R}{R_0}\right) \sin \alpha\right) = 0.8162 \quad (28)$$

$$\frac{R}{R_0} = 2.6415 \text{ but } R = 7.924 \text{ mm} \Rightarrow \Delta R = R - R_0 = 4.924 \text{ mm} \quad (29)$$

From (22)

$$4.924 \times 10^{-3} = (2.17 \times 10^{-3})^2 \frac{(0.7 - 0.144) \times 10^6}{E_b \times 0.67 \times 10^{-3}} \quad (30)$$

$$\Rightarrow E_b = 0.79359 \times 10^6 \text{ Pa} = 0.79359 \text{ MPa} \quad (31)$$

For avoiding failure of this system, the system should have 0.79359MPa Elastic modulus

$\Rightarrow$  For silicone rubber, the elastic modulus ranges from  $10^6$  to  $0.05 \times 10^9$

So this value is within the range

$$F = \frac{\pi R_0^2 P}{\sin^2 \alpha} (3(1 - \varepsilon)^2 \cos^2 \alpha - 1) \quad (32)$$

$$F = \frac{\pi R_0^2 P}{\sin^2 \alpha} \left( 3 \left( \frac{l}{l_0} \right)^2 \cos^2 \alpha - 1 \right) \quad (33)$$

But

$$\frac{l}{l_0} = \frac{\sqrt{1 - \left(\frac{R}{R_0} \sin\alpha\right)^2}}{\cos\alpha} \quad (34)$$

$$\Delta R = R - R_0 \Rightarrow R = R_0 + \Delta R \quad (35)$$

$$\frac{R}{R_0} = \frac{R_0 + \Delta R}{R_0} \quad (36)$$

$$\frac{l}{l_0} = \frac{\sqrt{1 - \left(1 + \frac{\Delta R}{R_0}\right) \sin\alpha}^2}{\cos\alpha} \quad (37)$$

$$\begin{aligned} 1 + \frac{\Delta R}{R_0} &= 1 + \frac{(2.17 \times 10^{-3})^2}{3 \times 10^{-3}} \frac{(P - P_{Th})}{0.79359 \times 10^6 \times 0.67 \times 10^{-3}} \\ &= 1 + \frac{8.85622 \times 10^{-9}}{3 \times 10^{-3}} (P - P_{th}) \\ \Rightarrow 1 + \frac{\Delta R}{R_0} &= 1 + 2.952 \times 10^{-6} (P - P_{th}) \end{aligned} \quad (38)$$

Substituting

$$\begin{aligned} \frac{l}{l_0} &= \frac{\sqrt{1 - \left((1 + 2.952 \times 10^{-6} (P - P_{th})) \sin\alpha\right)^2}}{\cos\alpha} \\ \Rightarrow \left(\frac{l}{l_0}\right)^2 &= \left(\frac{\sqrt{1 - (9.12218 \times 10^{-7} (P - p_{th}) + 0.3090)^2}}{0.9045}\right)^2 \\ &= \frac{1 - (8.3214 \times 10^{-13} (P - P_{th})^2 + 5.6375 \times 10^{-7} (P - P_{th}) + 0.0954)}{0.9045} \quad (39) \\ &= \frac{0.9045 - 5.6375 \times 10^{-7} (P - P_{th}) - 8.314 \times 10^{-1} (P - P_{th})^2}{0.9045} \\ \Rightarrow \left(\frac{l}{l_0}\right)^2 &= 1 - 6.2327 \times 10^{-7} (P - P_{th}) - 9.1918 \times 10^{-13} (P - P_{th})^2 \end{aligned}$$

Substituting this in Schulte's formula

$$F = \frac{\pi R_0^2 (P - P_{th})}{\sin \alpha} (3(1 - 6.2327 \times 10^{-7}(P - P_{th}) - 9.1918 \times 10^{-13}(P - P_{th})^2) \cos^2 18 - 1) \quad (40)$$

Pressures taken in this equation are ( $P - P_{th}$ ) because, to get effect contraction, initially braid and the inner tube should be in contact with each other

$$F = 2.96 \times 10^{-4}(P - P_{th})(1.713 - 1.6912 \times 10^{-6}(P - P_{th}) - 2.4942 \times 10^{-12}(P - P_{th})^2) \quad (41)$$

$$F = 5.0705 \times 10^{-4}(P - P_{th}) - 5.006 \times 10^{-10}(P - P_{th})^2 - 7.3828 \times 10^{-16}(P - P_{th})^3 \quad (42)$$

Required force per McKibben muscle to lift maximum load = 31.25N

Equating

$$31.25N = 5.0705 \times 10^{-4}(P - P_{th}) - 5.006 \times 10^{-10}(P - P_{th})^2 - 7.3828 \times 10^{-16}(P - P_{th})^3 \quad (43)$$

By solving this equation

$$\begin{aligned} (P - P_{th}) &= 508624.63Pa \\ \Rightarrow P &= P_{th} + 508624.63Pa = 0.144MPa + 0.508624MPa \\ P &= 0.652624MPa \end{aligned} \quad (44)$$

From the experiment using EMG sensors the maximum value of the EMG signal was found to be 453

$$\begin{aligned} P_{app} &= K \times EMG\ value \\ 0.652624MPa &= K \times 453 \\ \Rightarrow K &= 1440.671082Pa/unit \end{aligned} \quad (45)$$

From these values and equations, we will be able to find pressure which will likely give a motion similar to the hand movement.

- During the working of exosuit two important parts of actuation should be considered, one of them is the biceps muscle. A large part of force while doing some works is exerted by the biceps. Biceps muscle force calculation

is as shown above. Another important part of actuation is back muscle, we did the calculation for back muscle which is given below.

#### 4.2.3 Force and design calculation for back muscle

We decided to arrange back McKibben muscles at an angle of  $45^0$  between the spine and shoulder link to get proper actuation for shoulder joints.

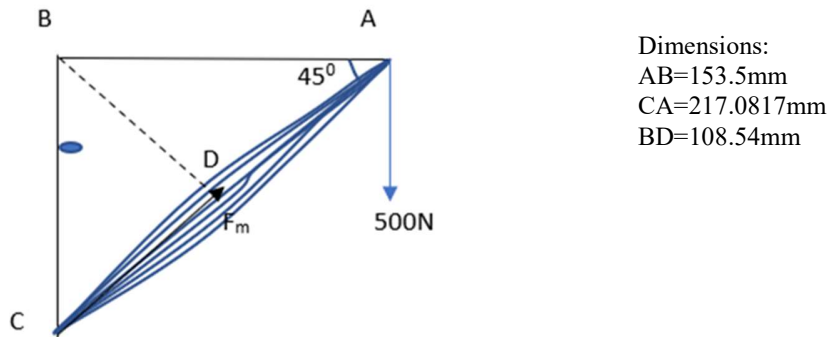


Figure 4.2 FBD of back muscle

Here we took our force requirement as 500N because the maximum capacity of our suit was decided to lift a load of  $2*25\text{kg}$ , by one hand. So from a rough estimate, this force would be same as the force that has to be exerted by tip of shoulder link, FBD of the back muscles considering the force requirement is given above.

From the FBD

Total force required by back McKibben muscle;

$$F_m = 500/\sin 45 = 707.106721\text{N} \quad (46)$$

The maximum force that a McKibben is limited to some value because McKibben muscle can withstand a maximum pressure of  $0.7\text{MPa}$ , so we decide the number of muscles accordingly.

Length of back McKibben muscle is  $217.0817\text{mm}$

The assumed Number of muscles in the bundle is 22

The maximum force required by a single filament

$$F_{single} = \frac{707.106721}{22} = 32.1412\text{N} \quad (47)$$

The equation (47) is based on assumption. In reality, the force exerted by a bundle of McKibben muscle will be less than the sum of the forces exerted by individual

fibers due to many losses non-rigidity of McKibben muscle and the unfilled gap between individual muscles.)

$$F = 5.0705 \times 10^{-4}(P - P_{th}) - 5.006 \times 10^{-10}(P - P_{th})^2 - 7.3828 \times 10^{-16}(P - P_{th})^3 \quad (48)$$

Substituting and solving

$$(P - P_{th}) = 0.5070683MPa \Rightarrow P = 0.6510683MPa \quad (49)$$

This pressure is the maximum pressure that we need to give to get the maximum force of 500N.

## CHAPTER 5

### DETAILED MECHANICAL DESIGN

#### **5.1 INTRODUCTION**

In this section, a detailed mechanical design of the suit was carried out. The computer-aided designing part was done using Autodesk Fusion 360 software. Before design, the mechanisms required to produce the required motion in exosuit were studied. Since human muscle augmentations are involved, we discussed the possibility of load-displacement from muscles to McKibben muscles were discussed, and the joints and their characteristics with a medical student. The axes of rotations, kinematic links required to produce effective motions in exosuits that mimic the anatomical motions of humans were derived before designing. The design of each element was derived by their motion restrictions and load-carrying capacity. The simplicity in design was given priority throughout the designing process.

The kinematic and dynamic modeling of one hand of exo-suit was done. DH modeling was used for kinematic modeling because this method can simply represent complex link systems. From the DH modeling, DH parameters were found which was later used as basic data for dynamic modeling. Transformation matrices for various frames which represent each link were also found, which could be used to get the position and orientation of different frames to the base frame. Dynamic modeling was done on Matlab with the help of a robot system tool. Representation of robot was done first with the help of rigidbodytree feature. Different links were added together and specified corresponding joints along with their mode of movement. Dynamic properties of each link were later added to get dynamic modeling. Different built-in were already available in the Matlab and with the help of those functions, different kind of dynamic and inverse dynamic analysis was carried out, that ultimately gave required torques for different motion, different motions for particular force and torque.

#### **5.2 MCKIBBEN MUSCLES**

The muscles were designed based on dimensions specified in theoretical calculations using Schulte's formula. A muscle bundle consists of several fibers the number of fibers required is decided by the force expectation of each muscle. A

fiber consists of an inner tube with an inner and outer diameter and a braided mesh with a specified braid angle surrounding the tube. The material used to make the inner tube is silicone rubber, and the outer fiber mesh is made using nylon. The material properties are specified in Appendix I.

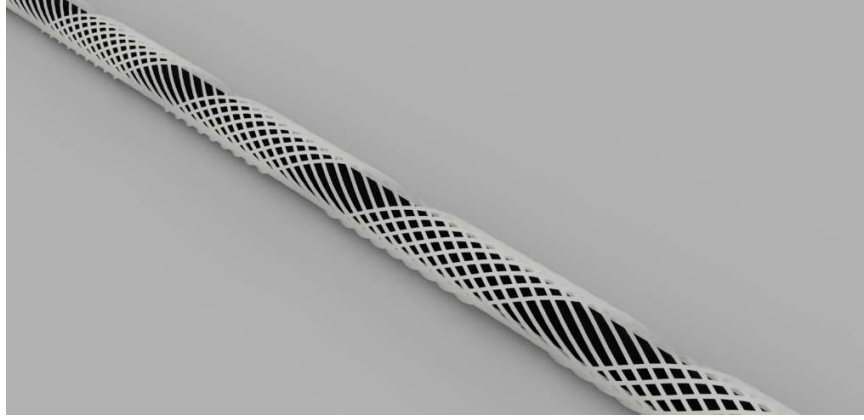


*Figure 5.1 CAD of McKibben muscle*

### 5.3 BACK COMPLEX

The back complex consists of the lumbar support structure. The lower part of the structure consists of a scissors mechanism which offers an added flexibility and effective load-carrying support and an element to hold the exoskeleton to our body. The upper part mainly consists of a spine-like structure that acts as a vertebra. The ends of both the biceps and back muscles are also attached to this structure. The material used for design and simulation purposes is two types of steel, Steel 60Sn40Pb and Stainless Steel AISI 202. Properties of this material are available in Appendix I.



*Figure 5.2: Back Complex*

<i>Area</i>	$3.065e+05 \text{ mm}^2$
<i>Density</i>	$7.852e-06 \text{ kg / mm}^3$
<i>Mass</i>	6.80 kg
<i>Volume</i>	$8.660e+05 \text{ mm}^3$

Table 5.1 Properties of Back

## 5.4 SHOULDER MECHANISM

The shoulder mechanism mainly consists of two parts, shown in Fig. 5.3, 5.4 which can perform shoulder internal and external rotation, abduction-adduction movement, and flexion-extension movement of the shoulder. Even though the effective axis of shoulder complex offsets from shoulder joint axis formed by shoulder girdle and ball and socket joints, simplicity in the design of shoulder complex was achieved. Using a set of three orthonormal axes will increase the complexity of the design and restraints range of motion of several components.

There are three joints in the shoulder complex,

- I. Rotational joint between back complex and part 1.
- II. Hinge joint between part 1 and part 2.
- III. Pined joint between part 2 and upper-limb (elbow complex).

All three joints collectively can produce the required motion on the shoulder joint.

Part 1 has a cylindrical component joined to the body due to this the stress concentration due to the discontinuity in the components was reduced. Part 2 has a pair of two cylindrical projections attached to it the reason is since hand-elbow carries most of the load applied to the suit these projections act as a cantilever beam providing more support to the upper-limb component. This projection also allows the upper limb to rotate. These two design decisions were made from structural analysis.



Figure 5.3: Part 1-Shoulder

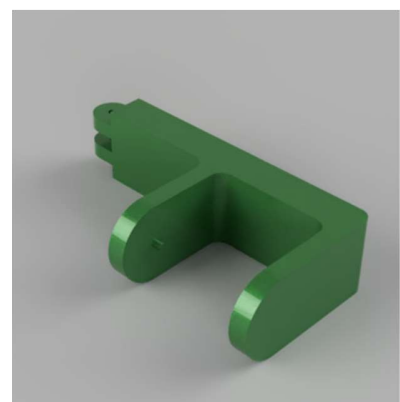


Figure 5.4: Part 2- Shoulder

Table 5.2: Properties of Part 1 and Part 2

<i>Part</i>	<i>1</i>	<i>2</i>	<i>2</i>
<i>Side</i>	<i>RHS &amp; LHS</i>	<i>RHS</i>	<i>LHS</i>
<i>Area /10<sup>4</sup> mm<sup>2</sup></i>	0.5993	1.828	1.828E
<i>Density/(10<sup>-6</sup> kg/mm<sup>3</sup>)</i>	7.85	7.850	7.850E-06
<i>Mass /kg</i>	0.129	0.558	0.558
<i>Volume /10<sup>4</sup> mm<sup>3</sup></i>	1.638	7.103	7.103
<i>Material</i>	<i>Steel AISI 4130 366 QT</i>	<i>Steel AISI 4130 366 QT</i>	<i>Stainless Steel AISI 202</i>

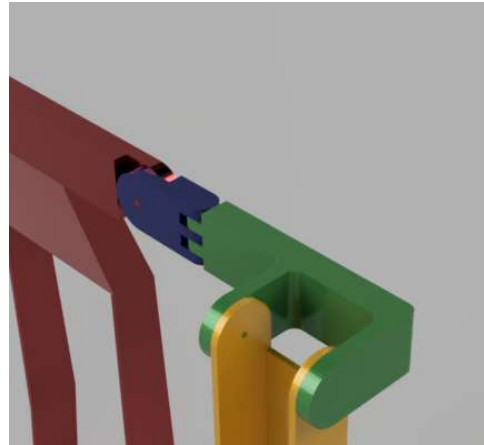


Figure 5.5: Shoulder Complex

## 5.5 ELBOW COMPLEX

The Elbow complex consists of three components, upper-limb, elbow-joint, and forearm. There are mainly two motions expected from the elbow complex; elbow flexion-extension and forearm pronation-supination. The components and complexes are designed accordingly to obtain these mechanisms. After structural analysis, several other factors such as strength requirement and wastage of materials were taken into consideration while designing the components. The range of motion requirement was also taken into consideration.

In elbow complex there are two joints;

- I. The pinned joint between upper-limb and elbow-joint
- II. The rational joint between elbow-joint and forearm



Figure 5.6: Upper-limb



Figure 5.7: Elbow-joint



Figure 5.8: Forearm-LHS



Figure 5.9: Forearm-RHS

The design of the left and right forearm structure differs because of the general antagonistic nature of the human arm. So to have a nominal range of motion in both arms while working together, both arms are designed differently.



Figure 5.10: Elbow-Complex

Table 5.3: Properties of components in elbow complex

<i>Part</i>	<i>Upper-limb</i>	<i>Upper-limb</i>	<i>Elbow-joint</i>	<i>Elbow-joint</i>	<i>Forearm</i>	<i>Forearm</i>
<i>Side</i>	<i>LHS</i>	<i>RHS</i>	<i>LHS</i>	<i>RHS</i>	<i>LHS</i>	<i>RHS</i>
<i>Material (Steel)</i>	<i>AISI 4130 366 QT</i>	<i>Stainless AISI 202</i>	<i>Stainless AISI 202</i>	<i>AISI 4130 366 QT</i>	<i>Stainless AISI 202</i>	<i>60Sn40Pb</i>
<i>Mass/g</i>	<i>735.145</i>	<i>735.587</i>	<i>1274.472</i>	<i>1273.706</i>	<i>2723.862</i>	<i>2722.497</i>
<i>Volume/ 10<sup>4</sup> mm<sup>3</sup></i>	<i>9.365</i>	<i>9.365</i>	<i>16.23</i>	<i>16.23</i>	<i>34.68</i>	<i>34.68</i>
<i>Density/ gmm<sup>-3</sup></i>	<i>0.008</i>	<i>0.008</i>	<i>0.008</i>	<i>0.008</i>	<i>0.008</i>	<i>0.008</i>
<i>Area/ 10<sup>4</sup> mm<sup>2</sup></i>	<i>5.982</i>	<i>5.982</i>	<i>3.735</i>	<i>3.735</i>	<i>8.290</i>	<i>8.288</i>

## 5.6 HAND COMPLEX

Hand complex is a complicated mechanism, this complex plays an important role in the displacement of the load to the exoskeleton and activation of sensors. The hand complex also provides mechanical support to the wrists.



Figure 5.11: Finger Complex

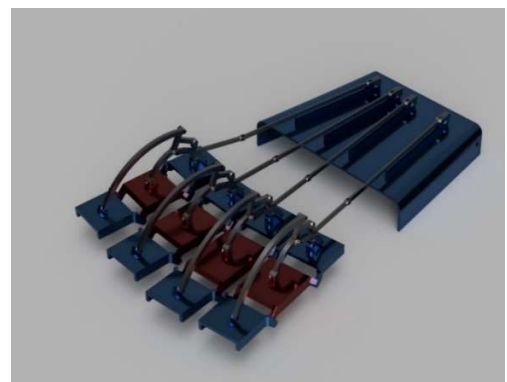


Figure 5.12: Hand Complex

The above figure shows a finger complex that has several components that can relatively rotate with one another at a small angle which enables slight flexibility in fingers while holding the weight. Such four-finger complexes are attached to a wrist part, a slider joint is present between these two parts which enable effective grip on the load and also provide effective distribution from fingers to the exoskeleton.

Table 5.4: Properties of hand complex

<i>Material</i>	Steel
<i>Mass</i>	167.855 g
<i>Volume</i>	2.138E+04 mm <sup>3</sup>
<i>Density</i>	0.008 g / mm <sup>3</sup>
<i>Area</i>	3.991E+04 mm <sup>2</sup>

## 5.7 EXOSKELETON

Combining all these mechanisms and complexes an exoskeleton was designed which has a load-carrying capacity of 50 kg. Also, muscular complex was designed according to the force requirement.



Figure 5.13: Muscles Complex

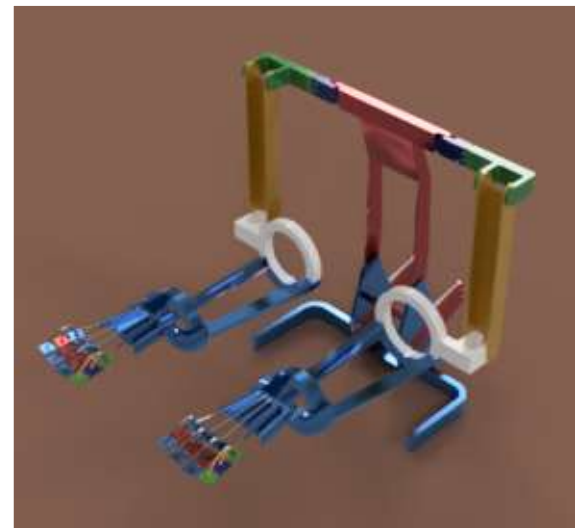


Figure 5.14: Exoskeleton

Combining the muscular complex (yellow in Fig 4.15) and the exoskeleton, an exosuit was designed which accompanies the sEMG sensors and the pneumatic tubes to the muscles.

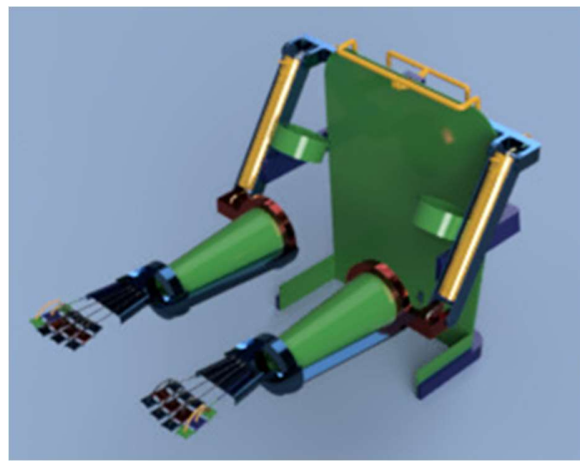


Figure 5.15: CAD model of Exosuit

Table 5.5: Properties of exoskeleton:

<i>Mass/g</i>	$1.798*10^4$
<i>Volume</i>	$2.289*10^6 \text{ mm}^3$
<i>Density</i>	$0.008 \text{ g / mm}^3$
<i>Area</i>	$7.951*10^5 \text{ mm}^2$
<i>Moment of Inertia at Center of Mass /10<sup>5</sup> g mm<sup>2</sup></i>	
<i>I<sub>xx</sub></i>	7189
<i>I<sub>xy</sub></i>	4.471
<i>I<sub>xz</sub></i>	-1.686
<i>I<sub>yx</sub></i>	4.471
<i>I<sub>yy</sub></i>	7647
<i>I<sub>yz</sub></i>	-522.1
<i>I<sub>zx</sub></i>	-1.686
<i>I<sub>zy</sub></i>	-522.1
<i>I<sub>zz</sub></i>	7152

## 5.8 KINEMATIC MODELING OF ARM

To do the dynamic modeling and corresponding motion analysis, we need to make the representation of the model. The simplest way to represent a model is by DH representation.

### **DH Modeling:**

The Denavit-Hartenberg (D-H) model of representation is a very simple way of modeling robot links and joints that can be used for any robot configuration, regardless of its sequence or complexity.

We assigned frames to each joint starting from 0 to 4. The parameters that were needed to find during the determination of DH parameters were the length of common normal  $d_n$ , the translational distance of x-axis along the z-axis  $a_n$ , angle of rotation of joints  $\theta_n$ , rotational angle of z-axis about x  $\alpha_n$ .

Z axes are taken along the axis of rotation starting from  $z_0$ , then x-axes were assigned which is either along the common normal or taken in the cross-product direction of intersecting z-axis. Y-axes are taken perpendicular to both x and z axes.

The reference axis is taken the same as the first frame to reduce complexity.

The next step was to find DH parameters for which we needed to consider four transformations which are given below.

1. Rotate about the  $z_n$ -axis an angle of theta  $(n+1)$ . This will make  $x_n$  and  $x_{n+1}$  parallel to each other. This is true because  $a_n$  and  $a_{n+1}$  are both perpendicular to  $z_n$ , and rotating  $z_n$  an angle of theta  $(n+1)$  will make them parallel (and thus, coplanar).
2. Translate along the  $z_n$ -axis a distance of  $d_{n+1}$  to make  $x_n$  and  $x_{n+1}$  colinear. Since  $x_n$  and  $x_{n+1}$  were already parallel and normal to  $z_n$ , moving along  $z_n$  will lay them over each other.
3. Translate along the (already rotated)  $x_n$ -axis a distance of  $a_{n+1}$  to bring the origins of  $x_n$  and  $x_{n+1}$  together. At this point, the origins of the two reference frames will be at the same location.
4. Rotate  $z_n$ -axis about  $x_{n+1}$ -axis an angle of  $\alpha_{n+1}$  to align  $z_n$ -axis with  $z_{n+1}$ -axis. At this point, frames  $n$  and  $n + 1$  will be the same and we have transformed from one to the next.

**Reference axes for this case:**

The reference axis is the same as the first frame to simplify the problem. If the reference frame and first are not the same then we also need to transform the reference frame to the first frame.

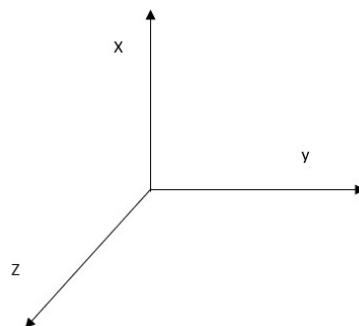


Figure 5.16 Reference axis

**DH representation:**

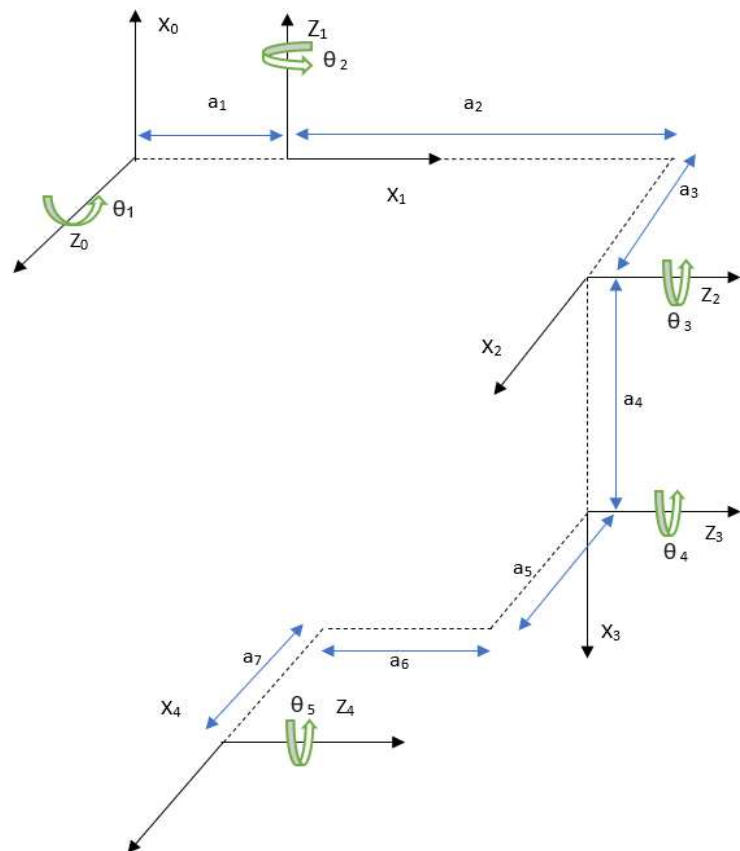


Figure 5.17 DH representation of one hand of our exosuit

**DH parameter table:**

DH parameters for each link were found from the transformations based on the DH representation. Each frame transformation represents the corresponding link between these two frames.

Table 5.6 DH parameter table

Link	$\Theta$	d	a	$\alpha$
<b>0-1</b>	$\theta_1-90$	0	$a_1$	-90
<b>1-2</b>	$\theta_2-90$	$a_2$	$a_3$	-90
<b>2-3</b>	$\theta_3+90$	0	$a_4$	0
<b>3-4</b>	$\theta_4-90$	$a_6$	$a_7 + a_5$	0

### 5.8.1 Drawing of the arm of exoskeleton

Drawing of the hand of exosuit with required dimensions to find DH parameters is shown below which is done by making drawing from the CAD model in solid works.

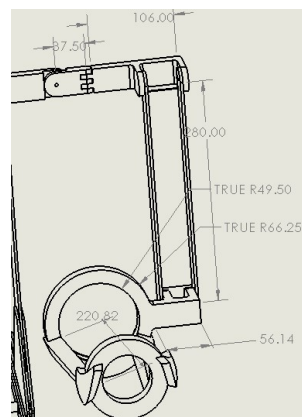


Figure 5.18 CAD of hand

### 5.8.2 Transformation matrices

Transformation matrices give the position and orientation of one frame for another frame. The general transformation matrix can be found from the multiplication of matrices which corresponds to respective steps in transformation.

So, the transformation matrix for the link from n to n+1

( From frame n to n+1)

$${}^nT_{n+1} = A_{n+1} = \text{Rot}(z, \theta_{n+1}) \times \text{Trans}(0,0, d_{n+1}) \times \text{Trans}(a_{n+1}, 0,0) \times \text{Rot}(x, \alpha_{n+1}) \quad (50)$$

$$A_{n+1} = \begin{bmatrix} C\theta_{n+1} & -S\theta_{n+1}C\alpha_{n+1} & S\theta_{n+1}S\alpha_{n+1} & a_{n+1}C\theta_{n+1} \\ S\theta_{n+1} & C\theta_{n+1}C\alpha_{n+1} & -C\theta_{n+1}S\alpha_{n+1} & a_{n+1}S\theta_{n+1} \\ 0 & S\alpha_{n+1} & C\alpha_{n+1} & d_{n+1} \\ 0 & 0 & 0 & 1 \end{bmatrix} \quad (51)$$

C⇒cos      S⇒sin

This general transformation matrix is used to determine the each transformations by substituting DH parameters into the matrix.

Transformation of frame 1-2

$$C_2=\cos \theta_2 \quad S_2= \sin \theta_2$$

$$A_1 = \begin{bmatrix} S_2 & 0 & C_2 & a_2S_2 \\ -C_2 & 0 & S_2 & -a_2C_2 \\ 0 & -1 & 0 & 0 \\ 0 & 0 & 0 & 1 \end{bmatrix} \quad (\text{angle is } \theta_1-90) \quad (52)$$

Transformation of frame 2-3

$$A_2 = \begin{bmatrix} S_3 & 0 & C_3 & a_3S_3 \\ -C_3 & 0 & S_3 & -a_3C_3 \\ 0 & -1 & 0 & a_4 \\ 0 & 0 & 0 & 1 \end{bmatrix} \quad (\text{angle is } \theta_2-90) \quad (53)$$

Transformation of frame 3-4

$$A_3 = \begin{bmatrix} -S_4 & -C_4 & 0 & -a_5S_4 \\ C_4 & -S_4 & 0 & a_5C_4 \\ 0 & 0 & 1 & 0 \\ 0 & 0 & 0 & 1 \end{bmatrix} \quad (\text{angle is } \theta_3+90) \quad (54)$$

Transformation of frame 4-5

$$A_4 = \begin{bmatrix} S_5 & C_5 & 0 & (a_6 + a_8)S_5 \\ -C_5 & S_5 & 0 & -(a_6 + a_8)C_5 \\ 0 & 0 & 1 & a_7 \\ 0 & 0 & 0 & 1 \end{bmatrix} \quad (\text{angle is } \theta_4=90^\circ) \quad (55)$$

Dimensions of the arm are noted from the drawing of the design which is given below.

$$\begin{aligned} a_1 &= 37.5\text{mm}, & a_2 &= 53 + 30 = 83\text{mm}, & a_4 &= 280\text{mm} \\ a_3 &= 42\text{mm}, & a_5 &= 52\text{mm}, & a_6 &= 74.269\text{mm}, \\ & & a_7 &= 240\text{mm} \end{aligned} \quad (56)$$

From these data, we can determine the total transformation matrix by the multiplication of all the matrices which gives us the position and orientation of the end effector to the reference frame. The first frame is the shoulder joint and the end effector is the wrist.

Total transformation is given by

$${}^0T_4 = A_1A_2A_3A_4 \quad (57)$$

- Using this matrix, position and orientation of wrist can be obtained to shoulder after substituting angle values and link lengths.
- The position of other Frames can be obtained by using different transformations calculated in the same way.  ${}^0T_1$ ,  ${}^0T_2$ ,  ${}^0T_3$

## 5.9 DYNAMIC MODELING OF EXO-SUIT

Dynamic modeling was done in Matlab using data from DH modeling and the design of exosuit. We used the rigid-body tree method in Matlab for the dynamic modeling of exosuit.

### Rigid body tree:

The rigid body tree is a representation of the connectivity of rigid bodies with joints. The rigid body tree in Matlab consists of rigid bodies, each rigid body can be added together by joints. The movement of joints should be specified like prismatic or revolute or fixed joints. Kinematic and dynamic modeling is possible if we specify the required properties to find these modelings. To do dynamic

modeling on Matlab we need to mention dynamic properties of each body like mass, the moment of inertia, the center of mass. We can also make a rigid body tree by defining DH parameters directly to Matlab

Table 5.7 DH parameter table:

Link	$\theta$	$d$	$a$	$\alpha$
0-1	$\theta_1-90$	0	$a_1$	-90
1-2	$\theta_2-90$	$a_2$	$a_3$	-90
2-3	$\theta_3+90$	0	$a_4$	0
3-4	$\theta_4-90$	$a_6$	$a_7+a_5$	0

### 5.9.1 Defining exo-suit hand in Matlab:

Steps involved in writing code

- The order of giving data to DH parameter matrix is  $a, \alpha, d, \theta$ .
- we have to define all the rigid bodies, then specify the transformations data for which is taken from the DH parameter matrix.
- Add each rigid body to the parent rigid body, define the joints which joint each link, specify the movement of each joint.

Robot: (5 bodies)

Idx	Body Name	Joint Name	Joint Type	Parent Name(Idx)	Children Name(s)
---	-----	-----	-----	-----	-----
1	body1	jnt1	revolute	base(0)	body2(2)
2	body2	jnt2	revolute	body1(1)	body3(3)
3	body3	jnt3	revolute	body2(2)	body4(4)
4	body4	body4_jnt	fixed	body3(3)	body5(5)
5	body5	jnt5	revolute	body4(4)	

Figure 5.19 Details of exo-suit hand in Matlab

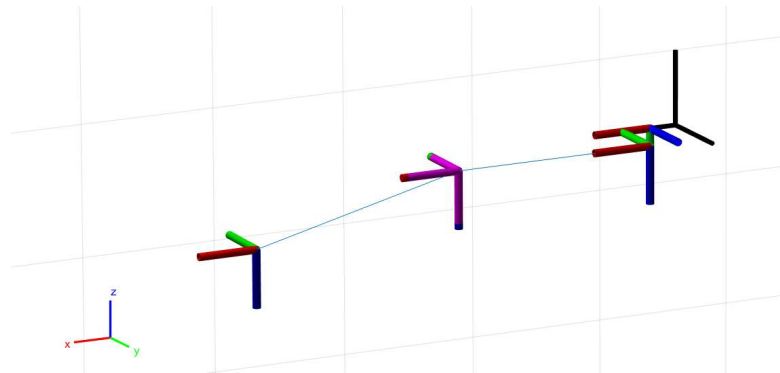


Figure 5.20 Diagram of exo-suit hand in Matlab

### Adding dynamic properties to links

To get the required torque to generate a particular motion, it is necessary to specify the dynamic properties of each link.

steps to specify dynamic properties:

- The data format should be selected as either row or column, here we selected the data format as a row and give the data as row matrices
- Mass is specified after body mass. Each link is assigned with its mass.
- The Center of mass is specified after the body. Center Of Mass, order of giving values is [  $x_c \ y_c \ z_c$  ]
- Moment of is specified after body. Inertia, the order of giving values of the moment of inertia is [  $I_{xx} \ I_{yy} \ I_{zz} \ I_{yz} \ I_{xz} \ I_{xy}$  ], These six independent moment of inertia should be given as input.

### Specifying joint velocity and acceleration

- Joint velocity and acceleration can be specified by setting data format to row and inserting respective values to a row vector.
- The number of values in the vector should be equal to the degree of freedom of the robot

#### 5.9.2 Results

##### Joint torques for static joint configuration:

inverse dynamics function can be used to calculate the required joint torques to statically hold a specific robot configuration.

- Specify the gravity in the row vector format

- Here a random configuration was generated and corresponding torques were determined using the in-built function for inverse dynamics

Joint angles:

1	2	3	4	5	6	7
-0.7203	1.3050	0.1948	-0.6252	2.6049	1.5746	0.3064

Joint torques:

1	2	3	4	5	6	7
4.4331e-16	-31.2101	1.7276	11.2035	0.3839	0.4174	0

Figure 5.21 output for static inverse dynamics

#### Joint torques to counter external force:

- External Force function was used to generate force matrices to apply to a rigid body tree model. Torques and forces applied to the body, specified as a [Tx Ty Tz Fx Fy Fz] vector.

Joint angles

1	2	3	4	5	6	7
1.8474	-1.7406	0.1854	1.2591	1.4171	-1.5009	-0.3794

Joint torques:

1	2	3	4	5	6	7
18.4934	103.6913	52.3250	84.3186	-23.0729	-59.7355	5.6843e-14

Figure 5.22 output for inverse dynamics with external force

#### Forward dynamics due to external force on the body:

Joint accelerations for a given robot configuration with applied external forces and forces due to gravity were found by using the forward dynamics function.

joint angles:

1	2	3	4	5	6	7
-0.6179	1.6147	-2.8408	1.4411	-1.2575	-1.0457	-0.0710

joint accelerations :

1	2	3	4	5	6	7
33.6785	57.3807	25.9125	-72.8191	12.6715	-7.5870	-0.0533

Figure 5.23 output for forwarding dynamics

# CHAPTER 6

## SENSING AND CONTROL

### 6.1 INTRODUCTION

In this section, the input signal acquisition methods and their control is discussed. An electromyogram (EMG) sensor will be used to obtain the input signal and Arduino Uno R3 will be used as our microcontroller. We have done an EMG signal acquisition test with a basic EMG circuit to obtain the muscle contraction and expansion values. Limitations were there due to the noise in the signal since basic gel electrodes were used in the test. A detailed study on the valve and compressor was also done for the controlling of the exoskeleton.

### 6.2 ELECTROMYOGRAM (EMG)

An electromyography (EMG) sensor is used for obtaining the input signal for our exosuit. A potential difference is created in the neurons of our muscle fibers as it contracts and expands, the EMG sensor continuously measures this potential difference across our muscle. Surface EMG electrode is used instead of needle electrode due to its non-invasive technique and simple setup. The AgCl gel electrodes are mostly preferred for obtaining the accurate value of EMG. The AgCl layer in the electrode allows current from the muscle to pass more freely across the junction between the electrolyte and the electrode. Thus, only a feeble electrical noise is introduced in the measurement.). It is important to obtain the EMG data in the low-frequency region also since some major information lies in this region. But since AgCl electrodes are expensive and difficult to procure we used normal gel electrodes in our test, even though there was noise in the signal the results were satisfying.

The best method for converting the filtered EMG signal into DC signals is by taking the Root Mean Square of a window of data points. An Arduino Uno microcontroller is used to convert AC to DC using the root mean square method.

$$RMS = \sqrt{\frac{1}{n} \sum_n x^2(t)} \quad (58)$$

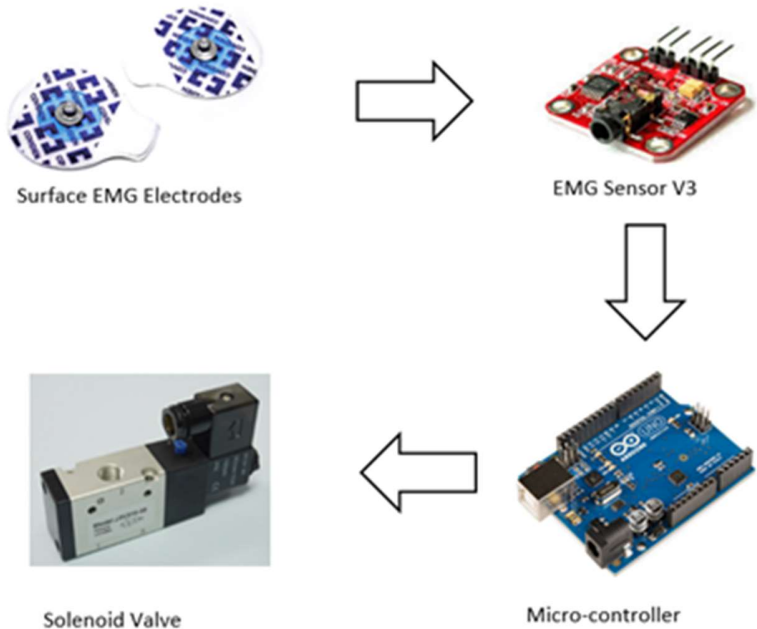


*Figure 6.1 Basic flow circuit*

### 6.3 EMG SIGNAL ACQUISITION

So with these references and literature study, we created our setup for EMG signal acquisition. The components of the circuit are

- Advancer technologies EMG Muscle Sensor V3
- Arduino Uno R3 (ATmega328)
- EMG Gel Electrodes
- MB102 Breadboard
- 9V Batteries
- Jumper wires

The aim was to obtain the EMG values for biceps contractions and extension, the test was carried out with one of the group members as the subject. The skin was properly cleaned before placing the EMG gel electrodes. Two electrodes were placed across the biceps muscle and the third electrode has to be placed on a bony area which serves as the reference electrode (Fig 6.3).

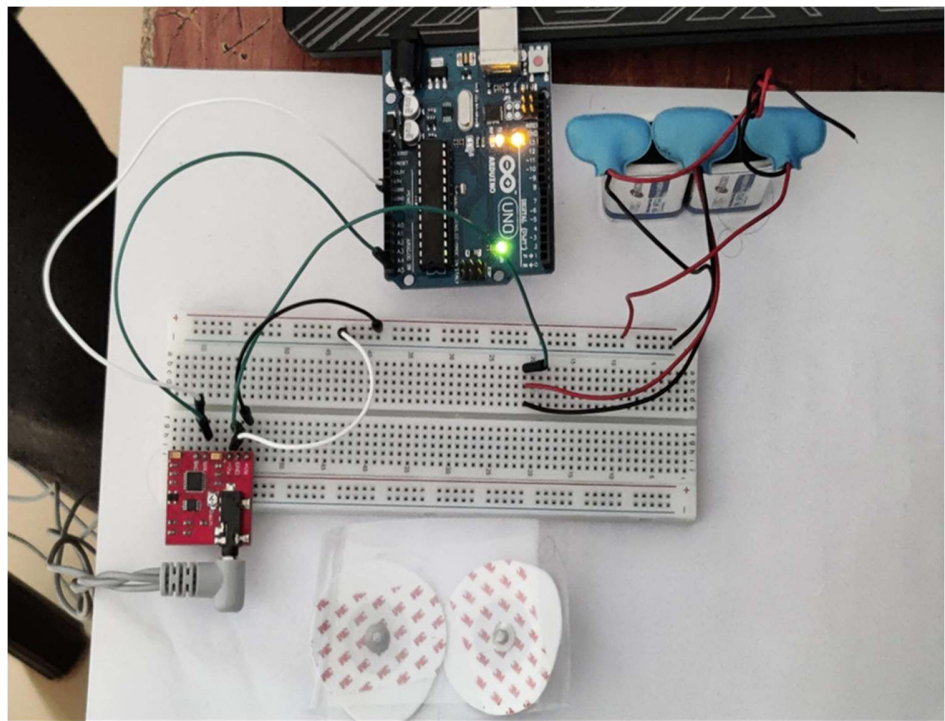


Figure 6.2 EMG circuit



Figure 6.3 EMG gel electrodes placed on the subject

Due to the high cost of AgCl electrodes and their less availability, we went with normal gel electrodes which introduced greater noise in the signal. The EMG sensor V3 that we choose has a good filtering bandwidth and decent amplification factor,

so it was able to produce a good rectified signal output. The Arduino Uno R3 was appropriately coded to obtain the RMS value of the signal.

#### 6.4 VALVES AND COMPRESSOR

There are different types of valve technologies available in the market Directional valve, proportional valve, servo valve, etc. But considering the cost factor and usage, we'll be using a 3/2 solenoid valve. In the de-energized state, the valve is closed and restricts the airflow from the compressor. When current is passed to the solenoid the coil gets energized and creates a magnetic field, which attracts the plunger against the spring force and thus opening the valve.

A 3/2 solenoid valve has 3 ports and 2 flow circuits. The three ports are connected to the compressor, multifilament muscle, and outside air. The two flow circuits are high-pressure airflow and outside airflow.

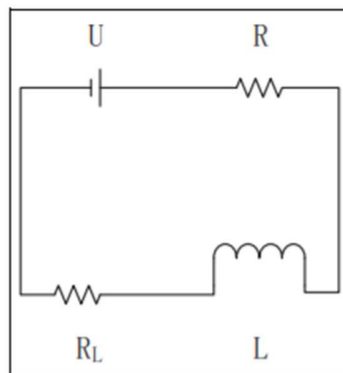


*Figure 6.4 Equivalent magnetic circuit*

The major drawback of this solenoid valve is slow response time which can be solved by making the tube connection between the valve and actuator short as possible to improve the dynamic response.

When the solenoid valve is energized and current passes through the circuit, the electromagnetic coil, and the power supply form a loop. We can obtain the circuit equation using Kirchhoff's law

$$i = \frac{U - N \frac{d\phi}{dt}}{R} \quad (59)$$

Where  $i$  is the current in the loop (Ampere),  $U$  is the supply voltage (Volt),  $N$  is the coil turns,  $\Phi$  is the coil flux (Wb) and  $R$  is the resistance of the electromagnetic coil (O).

As per our project requirement, HQC Tools 3/2 way Solenoid Valve 3V310-08 can be used. It has a working pressure in the range of 0.15-0.8 Mpa with a response time of 0.05s and power consumption of 3.5watt.

From the literature study, it is known that an average McKibben muscle cannot withstand pressure greater than 0.7Mpa. The minimum pressure is found by calculating the threshold pressure ( $P_{Th}$ )

Table 6.1  $P_{Th}$  VS Wall thickness of bladder:

X: Wall thickness (mm)	0.28	0.56	1
Y: $P_{th}$ (bar)	0.08	0.21	1.89

By linear regression we get

$$y = -0.321 + 2.63x \quad (60)$$

Putting the desired value of thickness  $x$ , and the minimum pressure required as 0.67 and 0.144 MPa respectively.

Therefore, the Range of pressure required is (0. 144, 0.7) MPa

Craftsman 5.6L air compressor can be selected due to its low weight and portability. It has a maximum pressure of 0.9 Mpa and a working pressure of 0.5 Mpa. This is an Oil-free pump, which requires minimal maintenance. Q235b steel housing structure gives this compressor more durability.

## **CHAPTER 7**

## **CONTROL**

### **7.1 INTRODUCTION**

In normal servo motor actuated exo-suits the control of the suit would be based on the control of torque delivered by the motor to the various joins attached to it. However, since the actuation method is based on pneumatics, pressure control of the actuator muscles is required which in turn provides the necessary torque required for active working of the exoskeleton. Multiple articles have been written focusing on the various types of control methodologies that can be implemented to monitor and coordinate the interactions between the user and system as well as the system and the environment. Despite the multitude of mechanisms available, the PID control is the most sought after due to its relative ease of design and tuning. In more advanced cases for better precision, an AFC scheme is implemented. In such an implementation, the AFC provides compensation for the noises and disturbances in the system that would have otherwise caused disruptions in smooth and efficient control. The price of such an inclusion is on the complexity of the system.

### **7.2 CONTROL LOGIC**

In this particular system, the sensor unit attached to the user picks up signals based on the user's activities and conveys them to the control unit working on an Arduino Uno that decides when the actuation should begin. The muscle activity recorded by the myograph during stressed muscular activity is compared continuously against standard muscle patterns that represent usual activity, like the unloaded movement of limbs or light loading like lifting a book. Only average readings can be taken as the noise that accompanies the values measured can often be misleading. Once a "threshold" pattern has been achieved the suit can be prompted to activate the artificial muscles to pressurize and aid the work of the user. Experimentation with commercial EMGs available has led to establishing a relationship between the voltages acquired and the load being lifted. However, the muscle output is seen to the top and shows a consistent pattern once a particular load level is reached. This urges the design of control that activates the muscles before the highest levels of

human muscle stresses are reached. Once this lower limit is crossed the suit is prompted to continuously provide pressure till the activity being done is taken over by the suit itself. The pseudo-code below shows the explained logic:

- *while ( $I_u > 0$ )*
  - {
  - if ( $I_u < L_h$ ) // when the load being moved is within human capability.*
  - {diff =  $L_h - I_u$*
  - Force is made proportional to the difference;*
  - Fa =  $K_1 * diff$ ;*
  - Force is applied till N is reached.*
  - }
  - else if ( $I_u = L_h$ ) // when the load is greater than or equal to the human capability*
  - { Fa =  $F_a + K_2 L_h$ ;*
  - break;*
  - }
  - }

### 7.3 PNEUMATIC CONTROL

Control of the pneumatic suit can also be attributed to the type of valve being used. In practice, a directional solenoid valve is used that although is cheaper than the other type offer only binary control, i.e, an ON/OFF situation. Control with such a setup would mean that when the sensor provides inputs that are greater than “threshold” values, the solenoid valve is activated to fully pressurize the muscles. In other words, the muscle is fully pressurized for every user activity between the threshold set and the suit's maximum stated limits.

On the other hand, using a proportional solenoid valve with PWM can give us better and continuous control. The control system can now be taught to understand the actuation requirements more accurately and the solenoid valve can now be made to make pressure adjustments so that, even after the lower threshold is crossed only

proportional amounts of artificial muscle expansion is made, which can then grow up to reach the maximum expansion to bear heavier loads. Thus the implementation of a proportional solenoid valve can give us a better range of control. The schematic below shows a hypothetical Simulink layout of the control which implements the above type of valve.

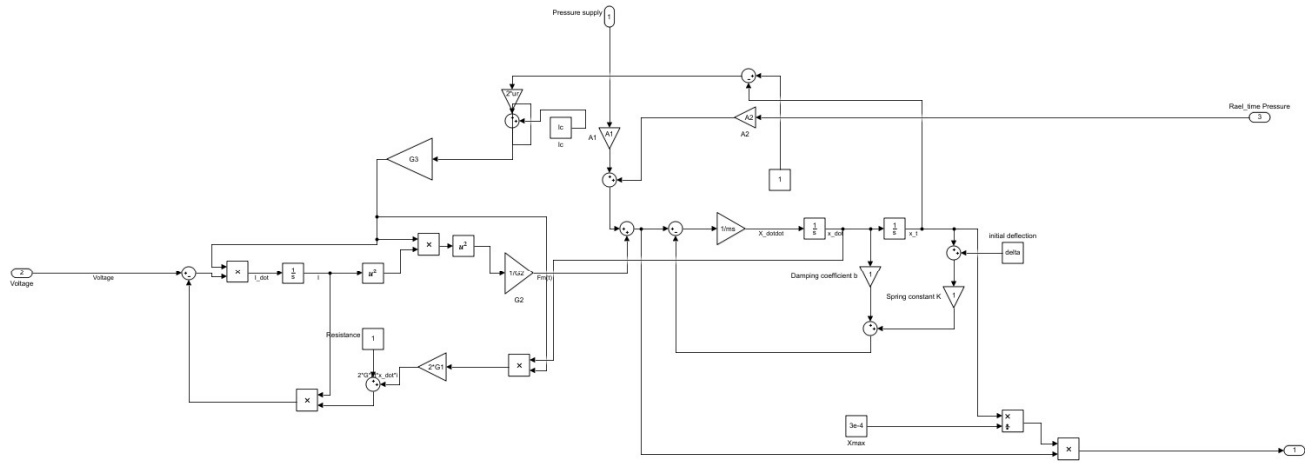


*Fig 7.1 Simulink block for proportional solenoid valve and pressure control*

The Simulink model takes input (Voltage) from the EMG sensor attached to the skin of the user and compares it to the standard values set by experimentation. The error generated ( $voltage$ ) works through a PID controller which transfers the corresponding voltage to the proportional solenoid and here the controller decided how much of the valve should open for air to flow out at a particular frequency (say 50 Hz). After the initial input voltage to current modeling, the circuit then makes use of the spool position in the solenoid as the control variable to dictate the percentage of pressurizing required. The pressure from the valve then based on the muscle model provides the force and torque required for actuation of the suit. A physical model of the suit works in unison with the remaining blocks to decide the parameters like limb velocity and position. The outputs from the blockwork in a negative feedback loop with the whole system form the complete control for the individual segments.

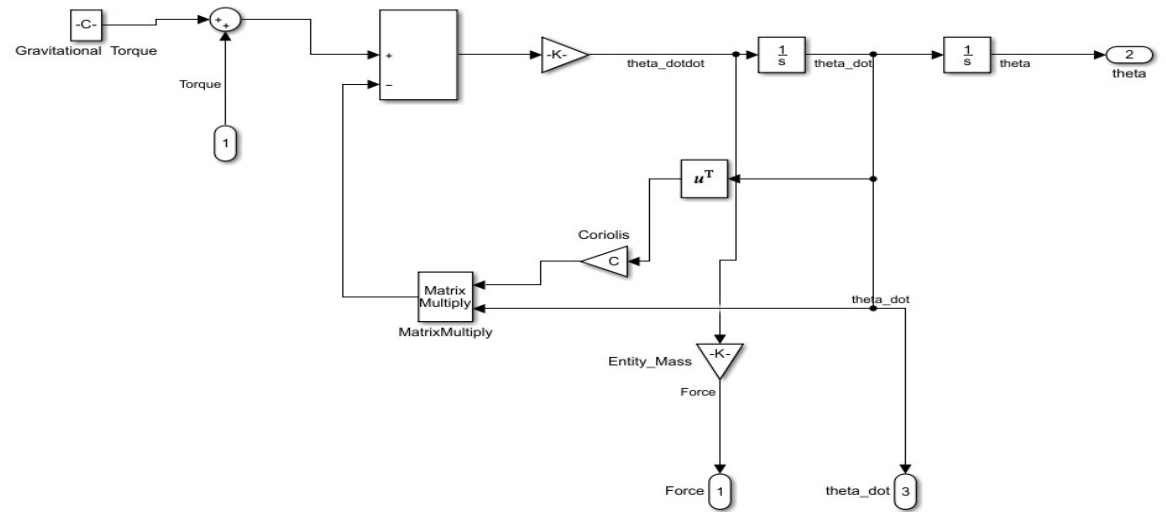


Fig 7.2 Simulink block of exo-suit physical model

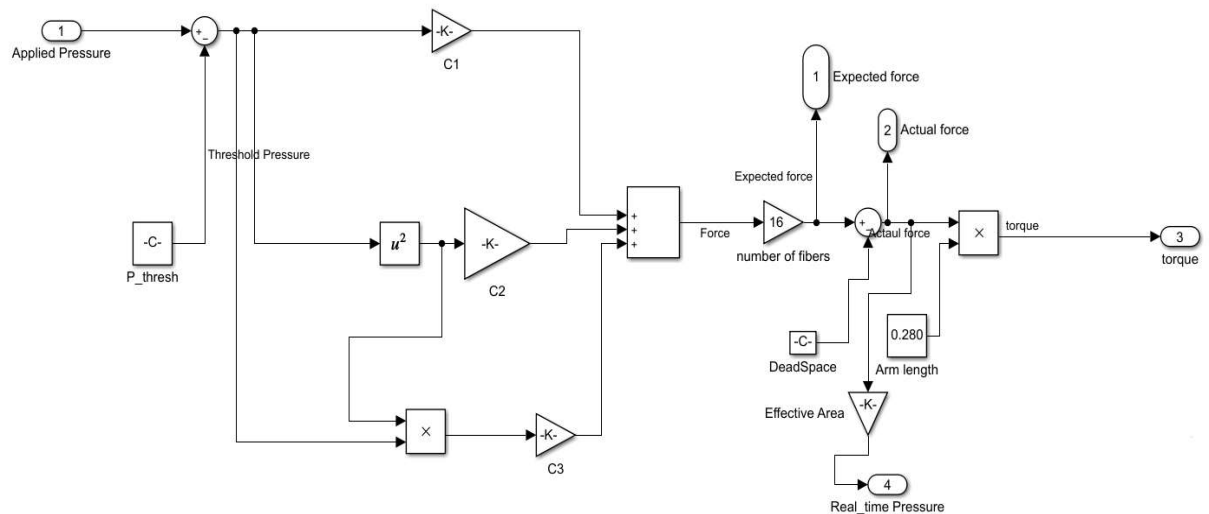


Fig 7.3 Simulink block for muscle model

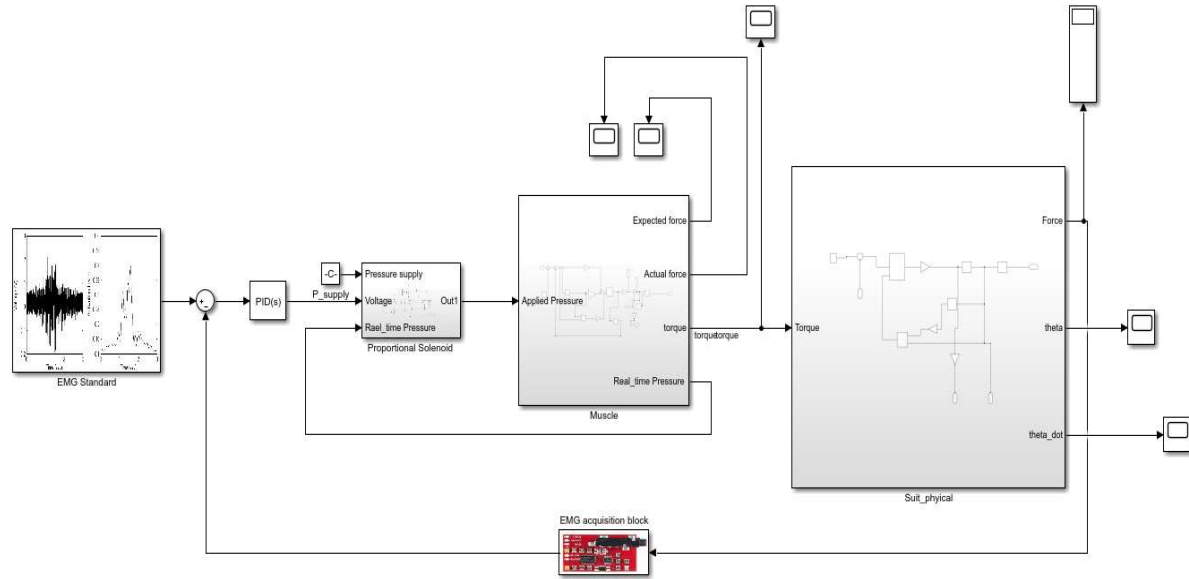


Fig 7.4 Overall Simulink system for suit control

The whole system can be made to work on an Arduino Uno where each muscle movement can be read by the corresponding EMG attached and from then on the consequential movement of different muscles can be achieved through a “Stack of Tasks” programming nodal implementation. Based on priority setting, each muscle group of the user under the EMG sensor can incite corresponding artificial muscles on the exo-suit to obtain a mimic behavior. Since multiple sensors will be present receiving muscle inputs a delay can be made to synchronize the entire artificial system to work in unison with the user.

#### 7.4 PID SCHEME

The controller works as mentioned before on a PID scheme, which provides real-time control. In our case it would be the difference in voltages between the standard EMG plot and the real-time EMG plot being fed in by the sensor unit, so:

$$evolatge = V_{desired} - V_{actual} \quad (61)$$

Further, the PID scheme can then be implemented to obtain the control signal;

$$U = K_p * e_{volatge} + K_i * \int e_{volatge} dt + K_d * \frac{d e_{volatge}}{dt} \quad (62)$$

The Simulink models are shown above work on a stock PID block which can be tuned by methods like the Zeigler Nicholas method or by experimenting and observing the time constant.

However, a basic PID setup can be seen below to see how the negative feedback into the PID helps in an “automatic” correction and arrival to require conditions. The transformation blocks are included so that required transfer functions can be incorporated.

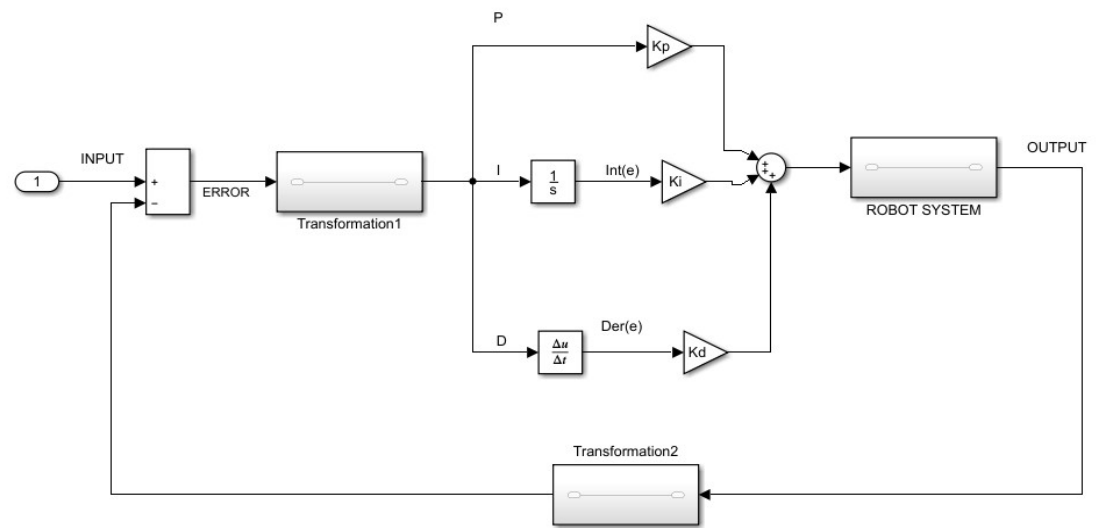


Fig 7.5 Schematic of a PID controller working with a robot system.

## CHAPTER 8

### RESULTS AND DISCUSSION

#### 8.1 RESULTS

The requirements of load-bearing suits that enable humans to expand their range of work have motivated the development of this suit. Several parameters that affect the modeling of the suit were studied and the design was made in accordance. Based on the numerical calculations and models made earlier the suit was designed and various tests were done on it to understand the extent of usage of the suit. Simulations were run on each segment to establish and understand sections where improvements can be made. The section that follows discusses the results obtained in this report

##### 8.1.1 Derivation of Braid Angle Relation in McKibben Muscles

While modeling the braid angle was observed to be the function of the length of the muscle fiber and twist angle, since other parameters such as tube diameters, fiber diameters are fixed. Twist angle is a design parameter that decides how much the fiber should turn around the tube to form an effective mesh. The dependency of braid angle on twist angle and length is shown in 8.1 and 8.2 respectively.

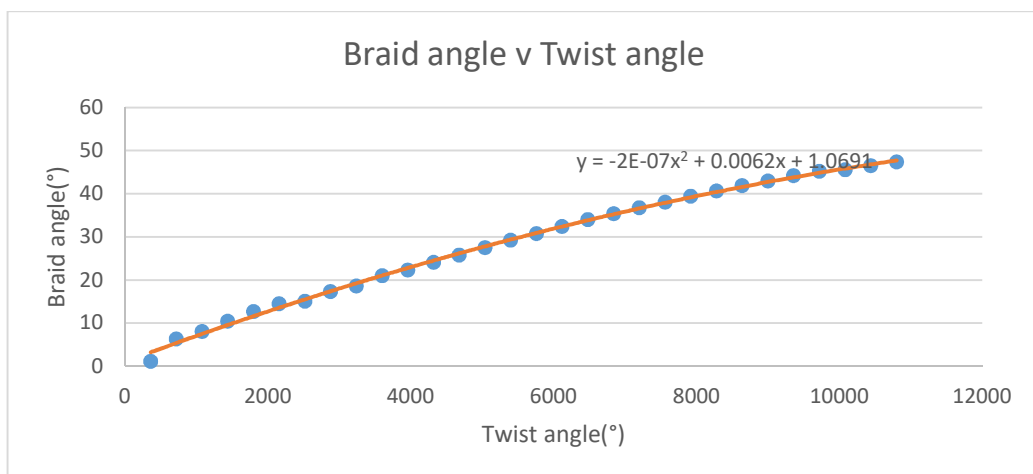


Figure 8.1: Graphical Relationship between Twist angle and Braid angle

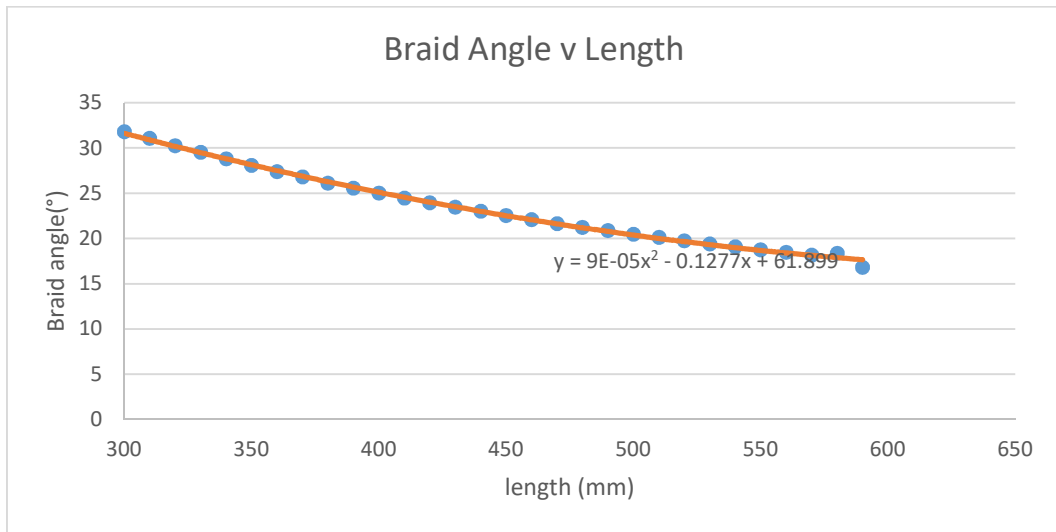


Figure 8.2: Graphical Relationship between Muscle length and Braid angle

From the graphs, a second-degree polynomial relationship with an increasing slope exists between twist angle and braid angle and the braid angle vs. length graph shows a negative slope. Using a statistical method, an empirical relationship was found between braid angle, twist angle, and length of the muscle.

$$\varphi = 9 \times 10^{-5}l^2 - 2 \times 10^{-7}\theta^2 + 0.1277l + 0.0062\theta + 42.295 \quad (63)$$

Where  $\varphi$  = Braid angle (°),  $l$ = length of the muscle (mm),  $\theta$ = twist angle (°). The error in the above equation is estimated at around  $\pm 0.986^\circ$  (Appendix II).

### 8.1.2 Statistical Structural Analysis

The structural analysis on various components exosuit was performed on maximum load condition. The simulation works were done on Fusion360 software, the factor of safety and the von mises stresses developed in various part of the exosuit is shown below. Due to the simplicity of the design, we were able to perform a simulation of the entire suit at once. The technical details of the simulation are provided in Appendix IV. The material was chosen based on the factor of safety requirements. A minimum factor of safety of 2.5 was maintained on the entire design. The main three materials used for design are Steels 60SnPb40, Stainless Steel AISI 202, and Steel AISI 4130 366 QT whose properties are provided in Appendix I. Even though the design components are similar on both RHS and LHS (except forearm), the distribution of forces is different on both sides. This is mainly due to the direction of momentum on the arm support and the slight difference in the design of the forearm.

### 8.1.2.1 Shoulder Complex

In the shoulder complex, two loads are directly applied to the structure to which assists in shoulder internal-external rotation and abduction-adduction motion. Besides these loads, moments, contact load, and reaction load from other components are also present in the shoulder complex.

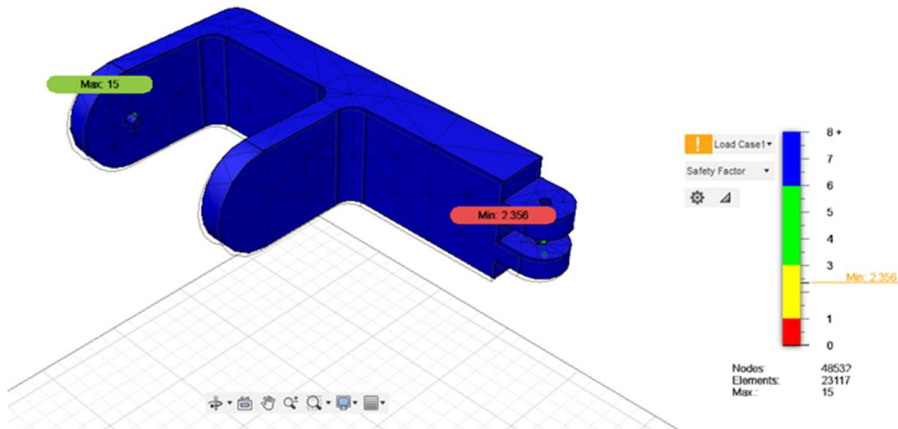


Figure 8.3: Factor of safety distribution in Part 2- SC (RHS)

This part is at a high tension compared to the other parts. This is because of the lesser stress distribution of other components of LHS (forearm and upper-limb). More load or stress is distributed to this part of the shoulder complex.

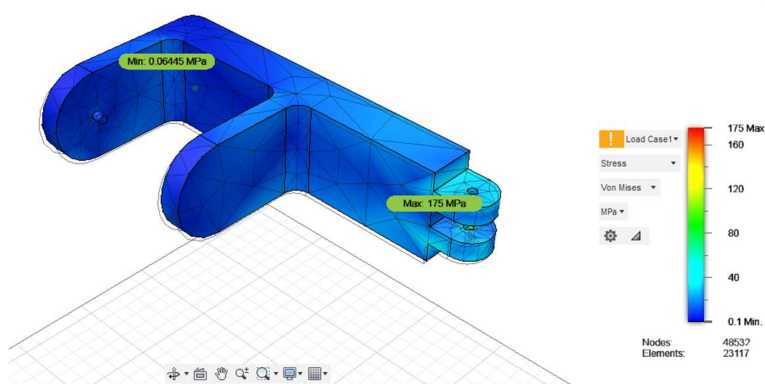


Figure 8.4: Von Mises Stress distribution in Part 2-SC (RHS)

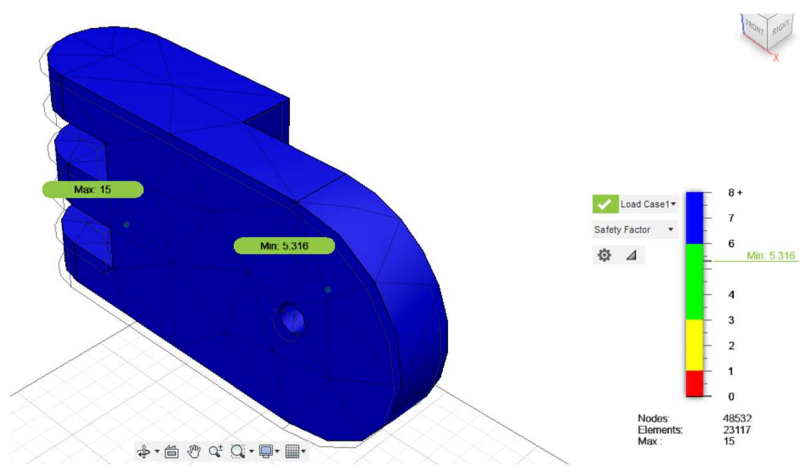


Figure 8.5: Factor of safety distribution in Part I- SC (RHS)

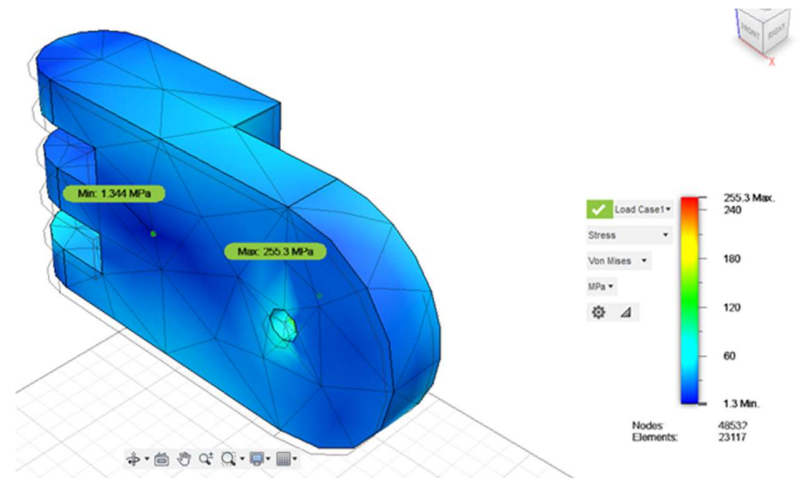


Figure 8.6: Von Mises stress distribution in Part I- SC (RHS)

Table 8.1: Simulation results: SC LHS

<i>Part</i>	<i>Maximum Stress/ MPa</i>	<i>Minimum FOS</i>
2	175	2.356
1	255.3	5.316

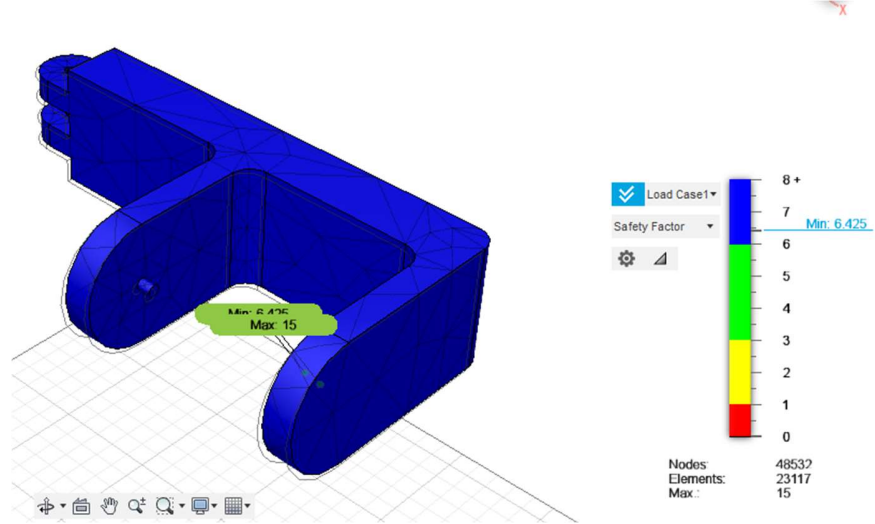


Figure 8.7: Factor of safety distribution in Part 2- SC (LHS)

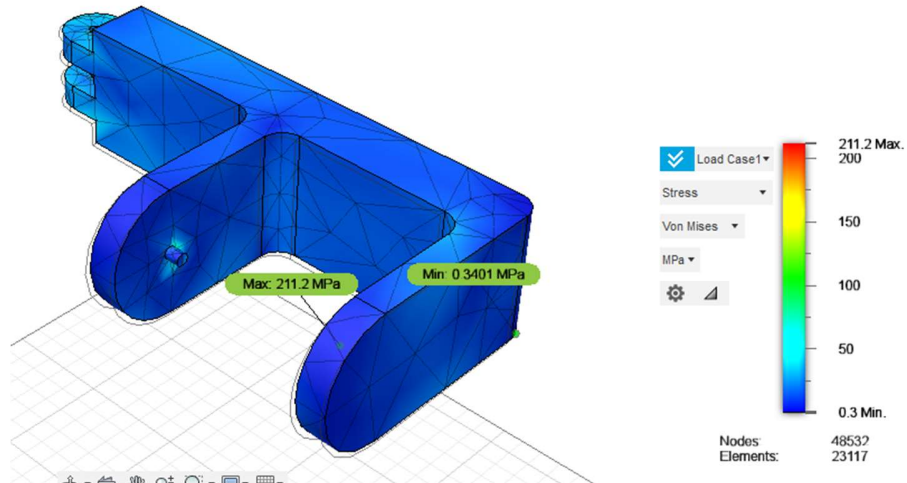


Figure 8.8: Von Mises stress distribution in Part 2- SC (LHS)

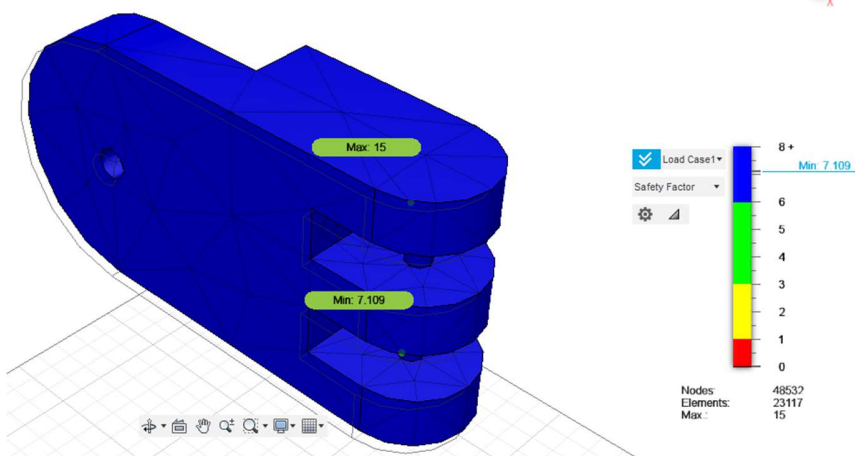


Figure 8.9: Factor of safety distribution in Part 1- SC (LHS)

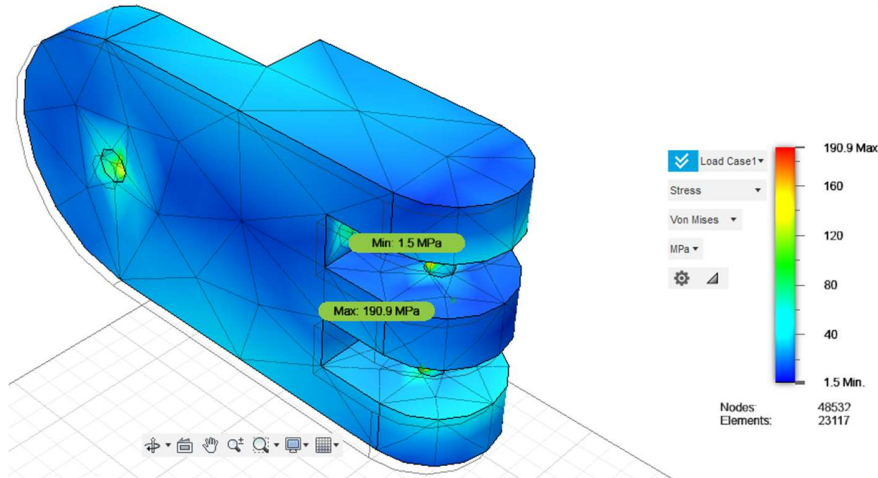


Figure 8.10: Von Mises stress distribution in Part 1- SC (LHS)

Table 8.2: Simulation results: SC- RHS

Part	Maximum Stress /MPa	Minimum FOS
2	211.2	6.425
1	190.9	7.109

### 8.1.2.2 Elbow Complex

In the elbow complex, the upper-limb part is more relaxed since there isn't any direct load applied to the component. The elbow joint part which connects the upper limb to the forearm has a direct load from McKibben muscle fiber attached to it. This set of muscle fibers play an important role in load carrying. The forearm comes directly in contact with the hand-complex which carries the weight. Hence a moment is observed in the forearm. Like SC, in the elbow, the RHS and LHS stress distribution differ. Materials used for each part design according to their strength requirement.

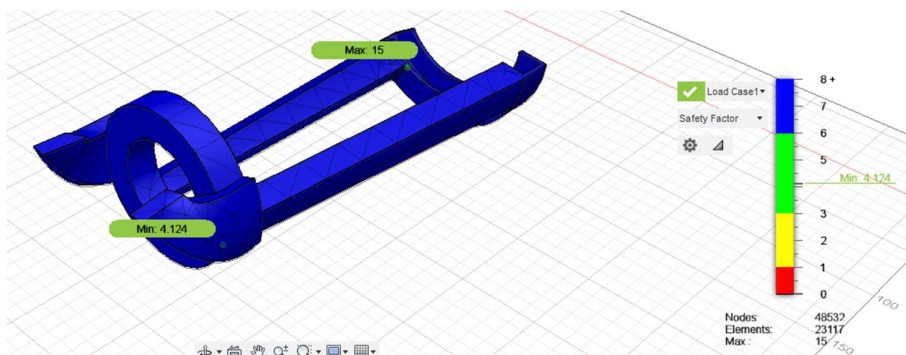


Figure 8.11: FOS distribution in the forearm- RHS

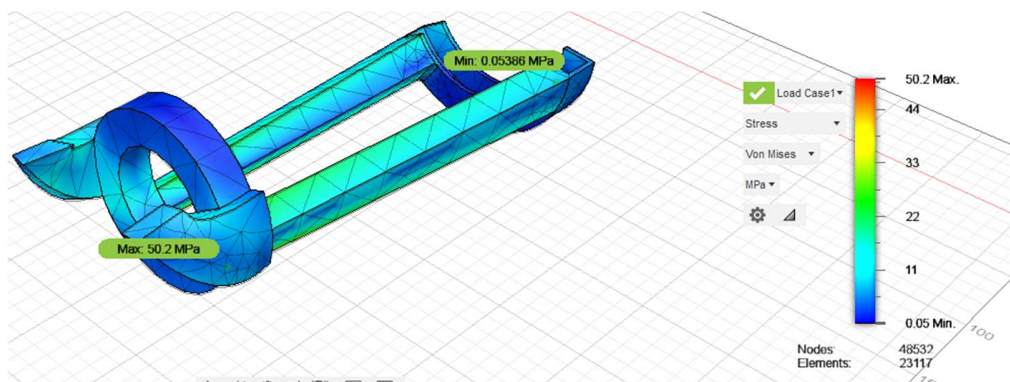


Figure 8.12: Stress Distribution in forearm-RHS

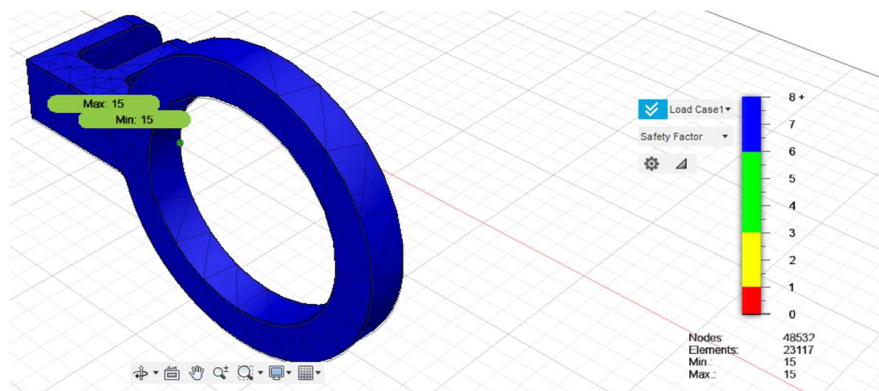


Figure 8.13: FOS distribution in elbow-joint- RHS

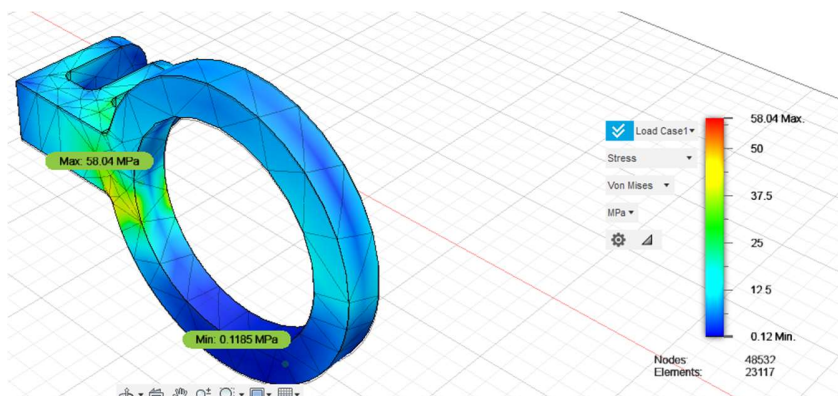


Figure 8.14: Stress DIstribution in elbow- joint- RHS

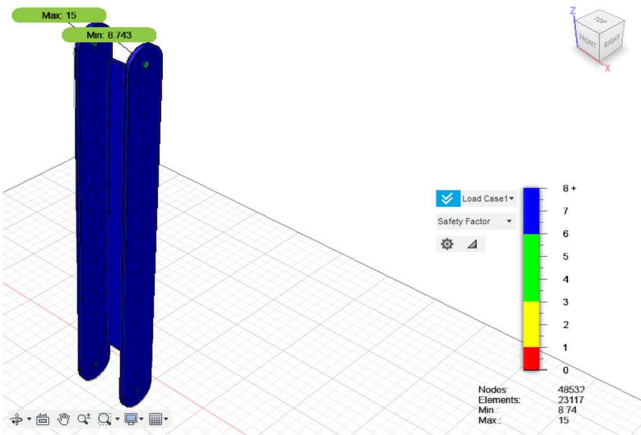


Figure 8.15: FOS distribution in Upper-limb RHS

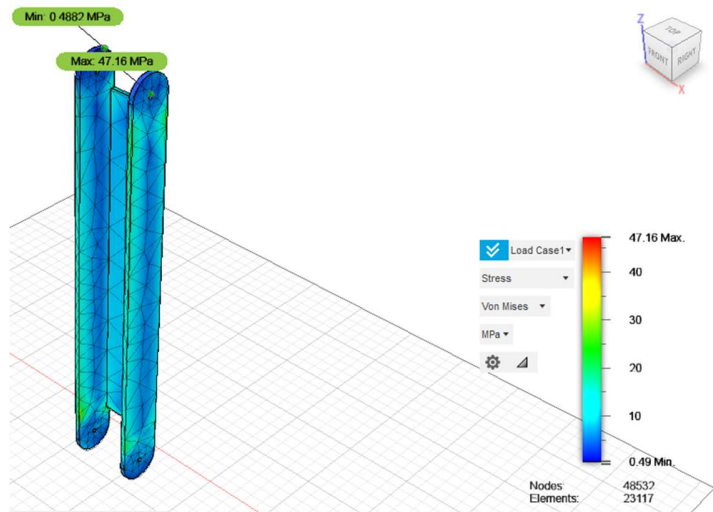


Figure 8.16: Stress distribution in Upper-limb RHS

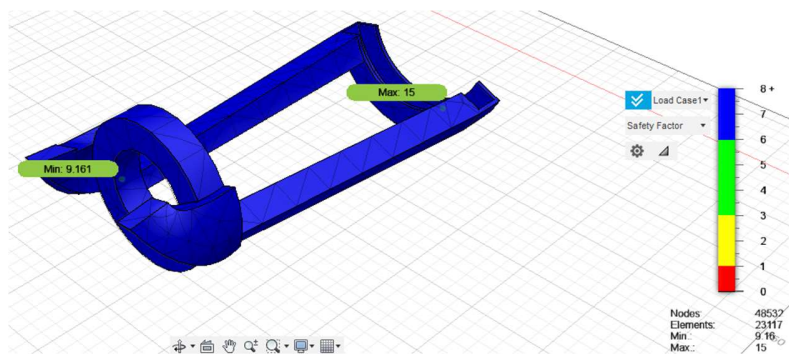


Figure 8.17: FOS distribution in forearm-LHS

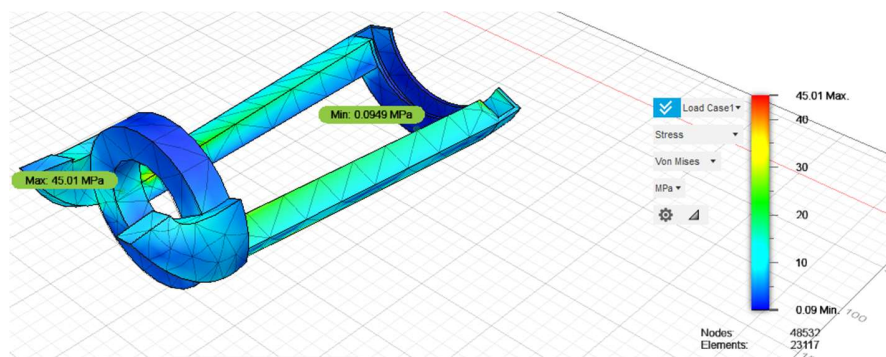


Figure 8.18: Stress Distribution in forearm-LHS

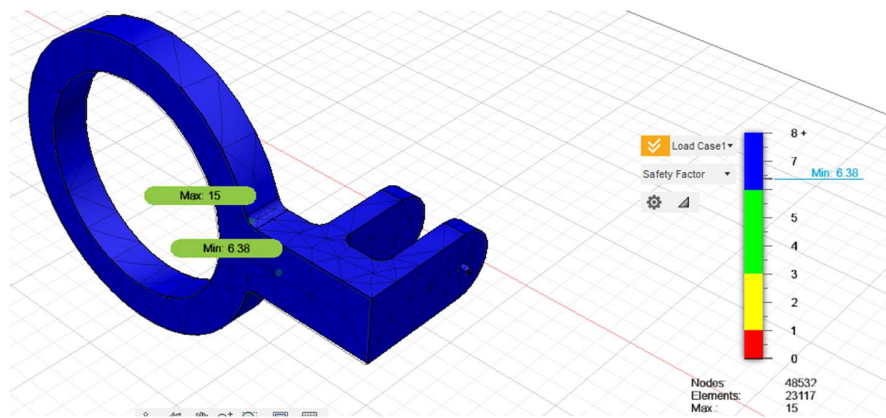


Figure 8.19: FOS Distribution in Elbow-joint LHS

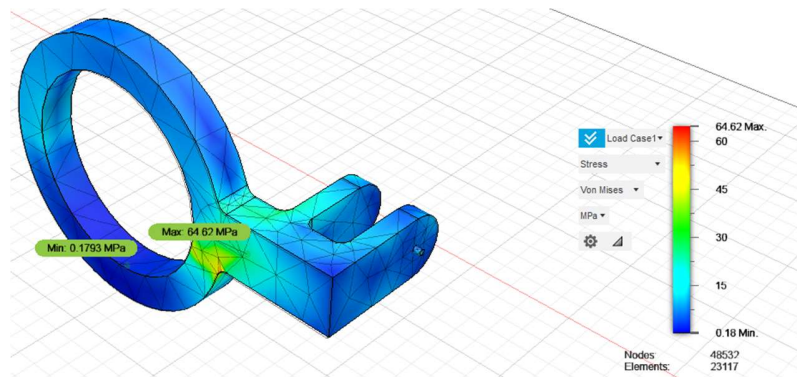


Figure 8.20: Stress Distribution in Elbow-joint LHS

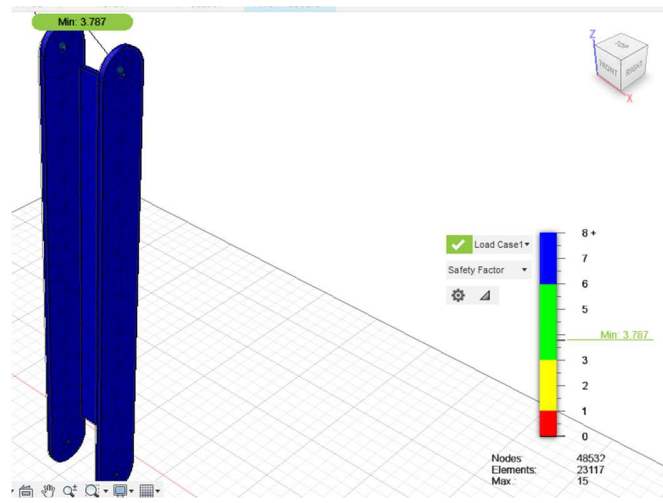


Figure 8.21: FOS Distribution in Upper-limb LHS

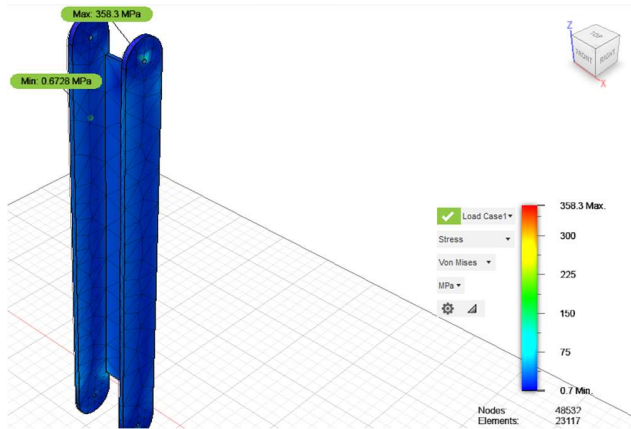


Figure 8.22: Stress Distribution in Upper-limb LHS

Table 8.3: Strength Analysis in Elbow Complex

Part	Side	Maximum Von Mises Stress /MPa	Minimum FOS
Forearm	LHS	45.01	9.161
	RHS	50.	4.424
Elbow-joint	LHS	64.02	8.36
	RHS	58.04	15
Upper-limb	LHS	358.3	3.757
	RHS	47.16	8.743

### 8.1.2.3 Back Complex

From the structural analysis of the Back Complex, it is observed that the back complex has the lowest FOS value. The back complex has several components of which the spine structure experiences the most stress. A load of the entire structure is displaced to the scissor mechanism in the back complex. Being an integral factor in the load-carrying capacity of the suit and providing mechanical support to the entire structure, the strength requirement in BC is expected to be very high.

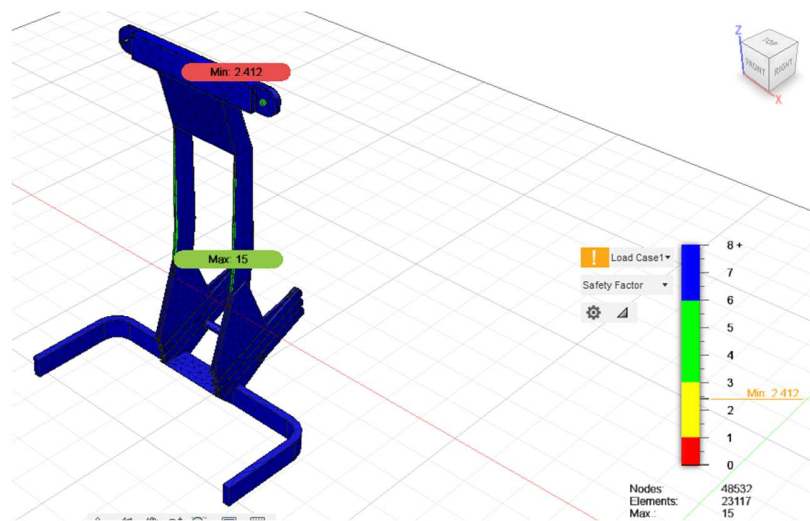


Figure 8.23: FOS distribution in Back Complex

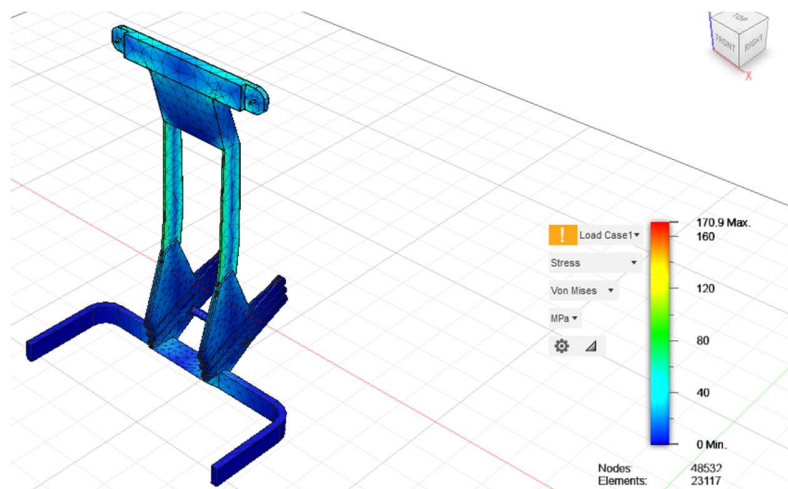


Figure 8.24: Stress Distribution in Back complex

Maximum Von Mises Stress = 170.9 MPa

Minimum FOS = 2.412

#### 8.2.1.4 Exoskeleton

Based on the load conditions, simulation of the entire assembly was done in Fusion360 and from the results, it was observed that the design is safe under maximum load condition with a minimum FOS value of 2.412. The structural analysis of the entire suit was conducted on the applied range of load, 0 to 50 kg.

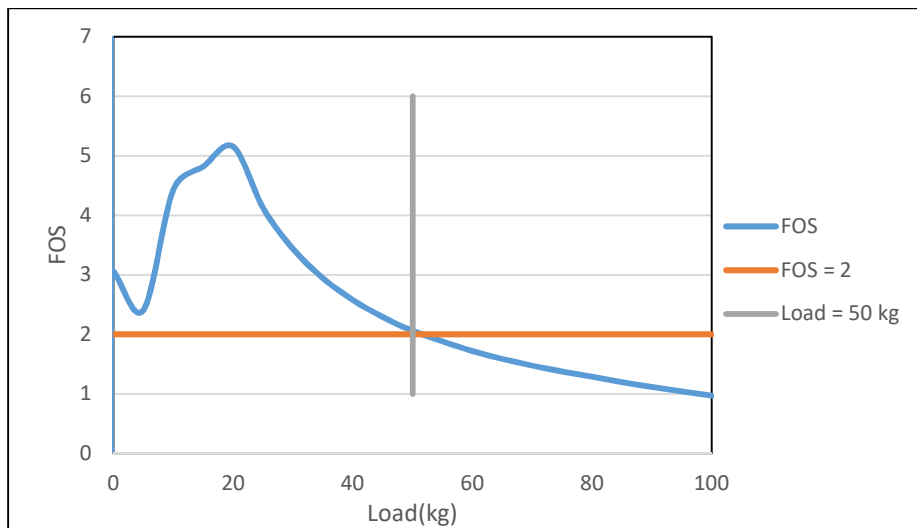


Figure 8.25: Variation of FOS w.r.t Load

.The study was made on the assumptions that back muscles are always engaged, hence the McKibben fibers which facilitate shoulder motions are fully engaged. Therefore the study is conducted by the varying load applied to the exoskeleton and support load offered by biceps McKibben fibers. The following graphs show the variation of different strength analysis parameter within the range of load applied to the exoskeleton.

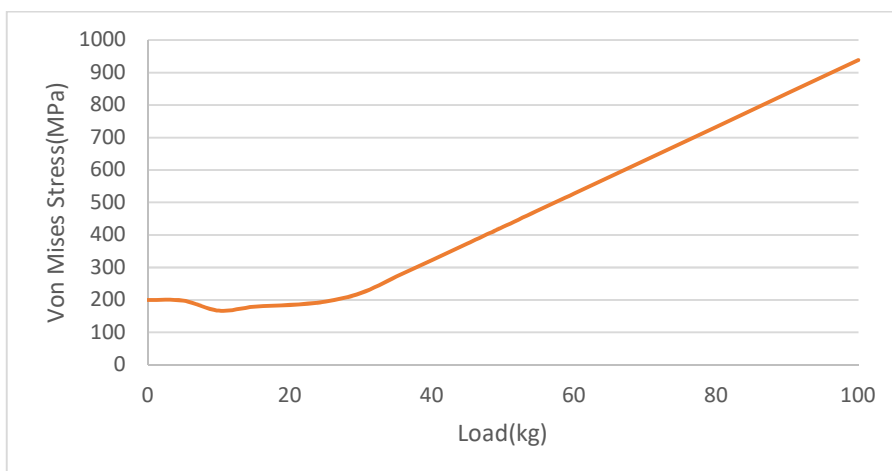


Figure 8.26: Variation in Stress w.r.t Load

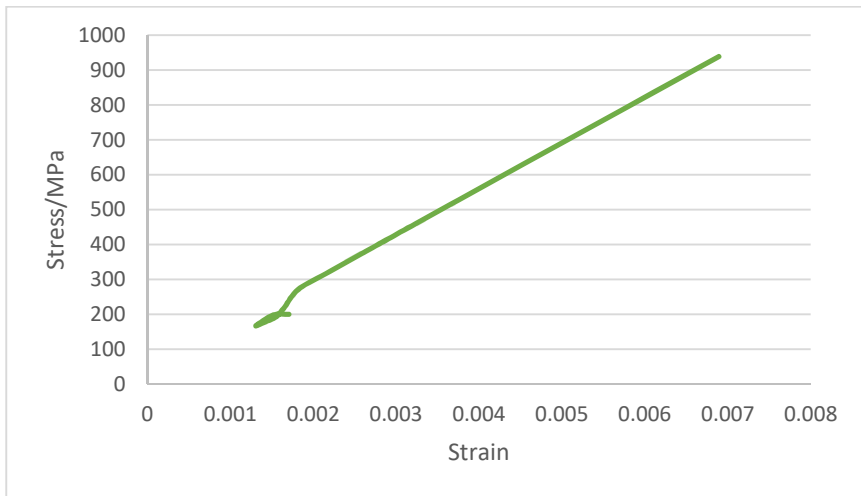


Figure 8.27: Stress-Strain Curve of the suit

From the graphs, we can conclude that our design is safe throughout our range of load (0-50 kg) ( $FOS > 2$ ). Strength wise the suit works at the best condition in between 15 to 30 kilograms ( $FOS > 4$ ). But when the structural analysis was done with maximum load condition, the load applied to the suit was 50 kg and the support offered by Biceps McKibben fibers are to be around 60 kgwt, to accommodate the weight of the suit and frictional losses. Back complex muscle fibers which assist in shoulder internal-external rotation will provide a maximum load of 100 N towards the back (since the range of motion to back from neutral positon is  $-20^\circ$ ). The fibers which assist in shoulder flexion-extension will provide a load of 500 N, considering all these factors simulation was done on the suit.

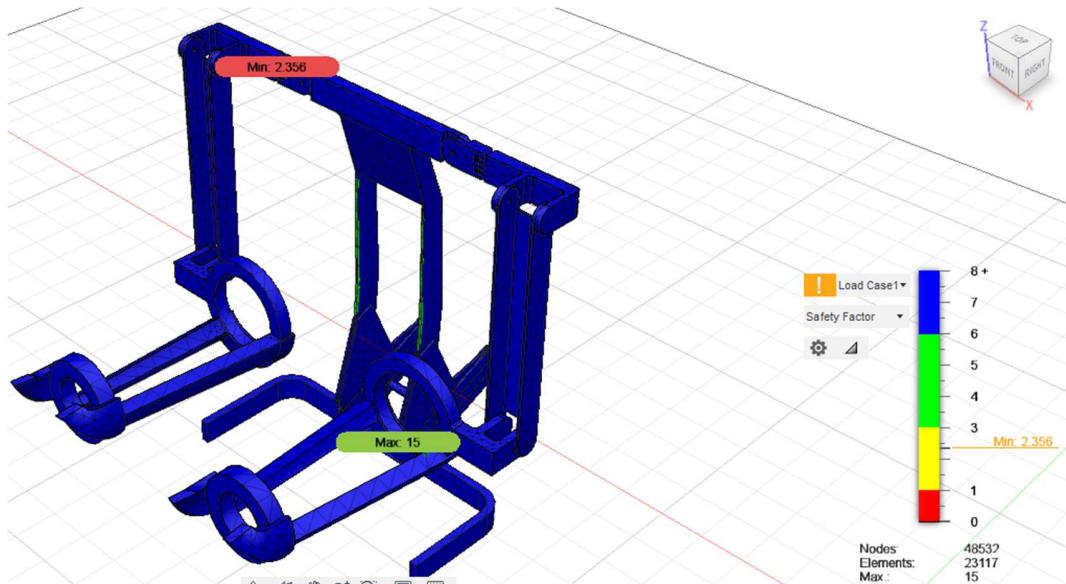


Figure 8.28: FOS Distribution in Exoskeleton

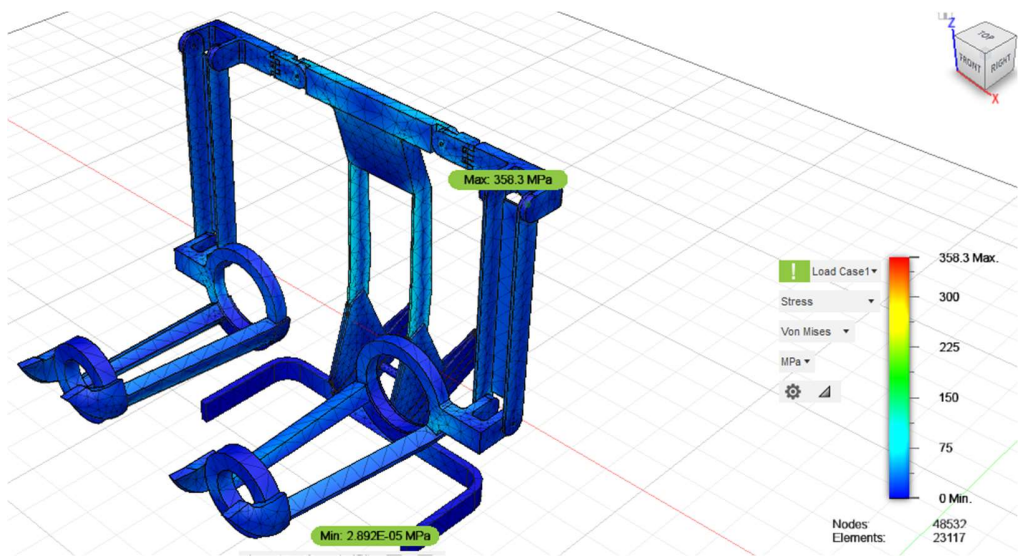


Figure 8.29: Stress Distribution in Exoskeleton

Table 8.4: Simulation results in Exoskeleton

Parameters	Minimum	Maximum
<i>Safety Factor</i>		
<i>Safety Factor (Per Body)</i>	2.356	15
<i>Stress</i>		
<i>Von Mises</i>	$8.617 \times 10^{-6}$ MPa	375.5 MPa
<i>1st Principal</i>	-190.9 MPa	248.9 MPa
<i>3rd Principal</i>	-597.2 MPa	89.06 MPa
<i>Total Displacement</i>	0 mm	4.012 mm
<i>Reaction Force</i>		
<i>Total</i>	0 N	1268 N
<i>X</i>	-121.6 N	102 N
<i>Y</i>	-286.8 N	415.6 N
<i>Z</i>	-1255 N	560.7 N
<i>Equivalent Strain</i>	$5.749 \times 10^{-11}$	0.002985
<i>Total Contact Pressure</i>	0 MPa	188.9 MPa

### 8.3 KINEMATIC AND DYNAMIC MODEL

- Kinematic modeling of our exo-suit hand was done and the used method for modeling was DH modeling.

- DH parameter table and transformation matrices for each link were computed
- Since our exosuit hand is a five-link mechanism, dynamic modeling by the Euler-Lagrangian method is very complex, so we decided to use Matlab robotic analysis for dynamic modeling
- Dynamic modeling was done with help of a robot system toolbox on Matlab and inverse and forward dynamic outputs were computed
- Outputs from Matlab dynamic modeling can be used for control of robot because it gives us the required torques to attain a particular motion

#### **8.4 CONTROL**

Control of the suit was done using a PID model with the valve being proportional. The control of the solenoid valve involves the control of the spool position, hence it is a combined model of both electrical and mechanical systems. This is seen to increase the complexity of the design as on many occasions the time required for computing is not within the simulations times and the model becomes limp. A memory block can be added however to counteract this and enable smooth functioning of the control. Since the user is well enveloped inside the exo-suit, sufficient care has to be taken so that even in case of failure the user leaves uninjured. As a safety precaution, the inclusion of a deadman's switch can aid in the immediate release of the user from the suit.

# CHAPTER 9

## CONCLUSION AND SCOPE FOR FUTURE WORK

### 9.1 CONCLUSION

An upper-body exoskeleton capable of augmenting the user load-bearing capabilities was designed and multifilament actuators were implemented as the power source of the suit.

The suit comprises a shoulder, elbow, forearm, and spine complex that works under the torque and force supplied by multifilament muscles.

Different sections throughout this report have analyzed the design from a different perspective and to conclude:

- The suit was designed from mathematical models and later on kinematic and dynamic analysis was done on it to see how well the suit works.
- CAD models of suit components and single muscle strand were designed and stress analysis was done on the same.
- A study of EMG sensing capabilities was done and a particular type of EMG unit was chosen as the sensor for user input.
- Further, a control system was designed that made use of continuous pressure control (pulse wave modulation) using appropriate valves.
- To work over the binary switching valves that are commonplace in pneumatic designs, a proportional solenoid valve was hypothesized to be used in the system.
- Finally, hardware attachments that add to the suit, the source of power, which is the compressor were studied and a suitable model was prescribed to the suit.

Few issues have been noticed during the entirety of this project:

- The concept of dead space present during the bundling of fibers reduces the expected force received.
- Although multiple EMG tests were conducted, the absence of precision sensors, in turn, affects the control of the suit. However, using proper AgCl coated electrodes has been seen to tackle this issue fairly.

- The use of an AFC control would have been able to tackle the noises that arise from the inputs as well as during the working cycle.
- Although the use of a proportional solenoid valve gives better control, the price of such an apparatus much higher than the conventional directional valves and increases complexity.

The solid structure of the exo-suit is designed to be made from three varieties of steel and the filaments are to be made from silicone rubber. Several rounds of testing were done to understand the extent of reliance on EMG signals and substantial results were seen. Several benefits have been seen in such a design, the suit seems to have better load capabilities than usual motor actuated designs of the same class. This can be attributed to the pneumatics involved in the system. Although heavier exoskeletons are available, the designed suit is expected to show higher degrees of flexibility and reduced bulkiness.

## **9.2 SCOPE FOR FUTURE WORK**

As talked about earlier, there are various segments of the suit that can be better designed or otherwise incorporated to achieve better results. At first, the design of the individual strands can be improved to achieve better force capabilities and different experiments can be conducted to reduce the reduction in force produced by the dead space between the fibers.

Although not proportional increasing the number of fibers in the bundle can improve the load-bearing capabilities. However, this might prove to be a challenge as increasing the fiber number might bring in weight to the suit. This then opens doors to research in better material choice, that while providing the required force still manages to be less heavy than its predecessors.

The entire suit at present requires an external power supply to allow the compressor to function. Providing a dense energy source on the suit might help in detaching the suit from a fixed location. However, unless the source is dense enough, the weight of the added source might prove to be a disadvantage. A more compact design might give sufficient range for improvements.

The biggest challenge for precision control is precise input acquisition. Using better EMG modules that have better-resolving strengths can help with this. EMG modules like Myo-wear can produce better results. Better experiments can be done to identify positions where the highest and clearest muscle signals are obtained from the body.

Although the control of the suit, based on a conventional PID scheme produce satisfactory results, in the future better control algorithms using machine learning or AI can be implemented so that the suit comes in unison with the wearer. Even with PID implementation, AFC schemes can be incorporated to make the control better. Experiments can be done conducted to see how the suit will fare against various working scenarios and different fields of work from factory assembly lines to advanced military uses.

## REFERENCES

- [1] Plagenhoef, S., Evans, F.G. and Abdelnour, T. “*Anatomical Data For Analyzing Human Motion*”. Research Quarterly for Exercise and Sport 54, pp.169-178. (1983)
- [2] M. H. Rahman, M. J. Rahman, O. L. Cristobal, M. Saad, J. P. Kenn'E and P. S. Archambault. “*Development of a Whole Arm Wearable Robotic Exoskeleton for Rehabilitation and To Assist Upper Limb Movements.*” *Robotica* (2015) Volume 33, Pp. 19–39.
- [3] Joel C. Perry, Jacob Rosen, Member, IEEE, and Stephen Burns. “*Upper-Limb Powered Exoskeleton Design*”. IEEE/ASME TRANSACTIONS ON MECHATRONICS, VOL. 12, NO. 4, AUGUST 2007.
- [4] R. Yupeng, P. Hyung-Soon and Z. Li-Qun, “*Developing a Whole-Arm Exoskeleton Robot with Hand Opening and Closing Mechanism for Upper Limb Stroke Rehabilitation,*” 2009 IEEE International Conference on Rehabilitation Robotics: Reaching Users & the Community (ICORR’09), Piscataway, NJ (Jun. 23–26, 2009)
- [5] Simon Christensen, Shaoping Bail, Sajid Rafique, Magnus Isaksson, Leonard O’Sullivan, Valerie Power, and Gurvinder Singh Virk “*AXO-SUIT - A Modular Full-Body Exoskeleton for Physical Assistance.*”. DOI: 10.1007/978-3-030-00365-4\_52.
- [6] Hiroyuki Nabae, Gen Endo, Shunichi Kurumaya “*Design of thin McKibben muscle and multifilament structure*”, Koichi Suzumori Department of Mechanical Engineering, Tokyo Institute of Technology, 2-12-1 Ookayama, Meguro-ku, Tokyo 152-8552, Japan.
- [7] Loris Roveda, Luca Savani, Sara Arlati Tito, Dinon Giovanni Legnani, and Lorenzo Molinari Tosatti “*Design Methodology of an Active Back-Support Exoskeleton with Adaptable Backbone-Based Kinematics*”. International Journal of Industrial Ergonomics 79 (2020) 10299.

- [8] Madeeha Majeed, Khurram Butt, Salman Qureshi, Bilal Majeed, 2013, “*Design and Control of Low- Cost Portable EMG Driven Exoskeleton Device for Human Wrist Rehabilitation*”, INTERNATIONAL JOURNAL OF ENGINEERING RESEARCH & TECHNOLOGY (IJERT) Volume 02, Issue 10 (October 2013).
- [9] A. Salman, J. Iqbal, U. Izhar, U. S. Khan and N. Rashid, "Optimized Circuit For EMG Signal Processing," 2012 International Conference of Robotics and Artificial Intelligence, Rawalpindi, 2012 IEEE
- [10] Nafiseh Ebrahimi, "Modeling, Simulation and Control of Robotic Arm", Department of Mechanical Engineering; the University of Texas at San Antonio
- [11] Musa Mailah, J RHewit,, Sheik Meeran,"Active Force Control Applied To A Rigid Robot Arm ", Jurnal Mekanikal, Jilid II, 1996
- [12] H. Kazerooni, S. L. Mahoney,"Force Augmentation in Human-Robot Interaction", American Control Conference San Diego, California, May 23-25, 1990
- [13] H. Rijpkema and M. Girard, “Computer Animation of Knowledge-Based Human Grasping,” in Proceedings of the 18th Annual Conference on Computer Graphics and Interactive Techniques (SIGGRAPH '91), pp. 339–348, 1991.
- [15] “*Modeling and Control of Mckibben Artificial Muscle Robot Actuators. Tmdu (Tondu Und Lapex-Nre with LESIA*”, Electrical and Computer Science Engineering Departement, INSA, Campus de Rangueil, 31077 Toulouse, France.
- [16] Sangian, D., Naficy, S., Spinks, G. M. & Tondu, B “*The effect of geometry and material properties on the performance of a small McKibben muscle system,*” (2015). Sensors and Actuators, A: Physical, 234 150-157.

**APPENDIX I**  
**PROPERTIES OF THE MATERIALS USED**

Material	Silicone rubber	Nylon 6	Steel 60Sn40P b	Stainless Steel AISI 202	Steel 4130 366 QT
Density/g/cm <sup>3</sup>	1.25	1.12	7.850	7.855	7.85
Young's Modulus / GPa	1.007	2.758	210	204.773	207
Poisson's Ratio	0.49	.35	0.3	0.29	0.33
Yield Strength/ MPa	10.34	70.4	207	412.304	1357
Ultimate Tensile Strength/ MPa	10.34	75.7	345	667.409	1426
Shear Modulus/ GPa	$1.007 \times 10^{-3}$	1	80	79.98	77.82

**APPENDIX II**  
**ERROR CALCULATION FOR EMPIRICAL FORMULAE TO OBTAIN BRAID ANGLE**  
 $l = 500 \text{ mm}$

Sl. No.	$\theta$	$\varphi$	$\hat{\varphi}$	$\varphi - \hat{\varphi}$	$(\varphi - \hat{\varphi})^2$
1	360	1.1285	3.15108	2.02258	4.09083
2	720	6.322	5.30532	-1.01668	1.033638
3	1080	8.0635	7.40772	-0.65578	0.430047
4	1440	10.437	9.45828	-0.97872	0.957893
5	1800	12.7135	11.457	-1.2565	1.578792
6	2160	14.493	13.40388	-1.08912	1.186182
7	2520	15.1045	15.29892	0.19442	0.037799
8	2880	17.325	17.14212	-0.18288	0.033445
9	3240	18.602	18.93348	0.33148	0.109879
10	3600	21.0125	20.673	-0.3395	0.11526
11	3960	22.3195	22.36068	0.04118	0.001696
12	4320	24.106	23.99652	-0.10948	0.011986
13	4680	25.766	25.58052	-0.18548	0.034403
14	5040	27.4625	27.11268	-0.34982	0.122374
15	5400	29.212	28.593	-0.619	0.383161
16	5760	30.7115	30.02148	-0.69002	0.476128
17	6120	32.3905	31.39812	-0.99238	0.984818
18	6480	33.9825	32.72292	-1.25958	1.586542
19	6840	35.3795	33.99588	-1.38362	1.914404
20	7200	36.7405	35.217	-1.5235	2.321052
21	7560	38.0095	36.38628	-1.62322	2.634843
22	7920	39.379	37.50372	-1.87528	3.516675
23	8280	40.628	38.56932	-2.05868	4.238163
24	8640	41.833	39.58308	-2.24992	5.06214
25	9000	42.949	40.545	-2.404	5.779216
26	9360	44.154	41.45508	-2.69892	7.284169
27	9720	45.196	42.31332	-2.88268	8.309844
28	10080	45.535	43.11972	-2.41528	5.833577
29	10440	46.464	43.87428	-2.58972	6.70665
30	10800	47.366	44.577	-2.789	7.778521

$$\begin{aligned}\varphi &= -2 \times 10^{-7} \theta^2 + 0.0062\theta + 1.0691 \\ \text{SSE} &= 74.554 \\ \text{MSE} &= 2.663 \\ u(\varphi)_0 &= 1.631^\circ\end{aligned}$$

Sl. No.	1	$\varphi$	$\hat{\varphi}$	$\varphi - \hat{\varphi}$	$(\varphi - \hat{\varphi})^2$
1	300	31.7945	31.813	0.0185	0.000342
2	310	31.0595	31.085	0.0255	0.00065
3	320	30.238	30.375	0.137	0.018769
4	330	29.518	29.683	0.165	0.027225
5	340	28.8	29.009	0.209	0.043681
6	350	28.084	28.353	0.269	0.072361
7	360	27.39	27.715	0.325	0.105625
8	370	26.789	27.095	0.306	0.093636
9	380	26.1155	26.493	0.3775	0.142506
10	390	25.564	25.909	0.345	0.119025
11	400	25.004	25.343	0.339	0.114921
12	410	24.466	24.795	0.329	0.108241
13	420	23.95	24.265	0.315	0.099225
14	430	23.47	23.753	0.283	0.080089
15	440	22.9965	23.259	0.2625	0.068906
16	450	22.545	22.783	0.238	0.056644
17	460	22.099	22.325	0.226	0.051076
18	470	21.6495	21.885	0.2355	0.05546
19	480	21.239	21.463	0.224	0.050176
20	490	20.863	21.059	0.196	0.038416
21	500	20.477	20.673	0.196	0.038416
22	510	20.112	20.305	0.193	0.037249
23	520	19.7535	19.955	0.2015	0.040602
24	530	19.3915	19.623	0.2315	0.053592
25	540	19.079	19.309	0.23	0.0529
26	550	18.751	19.013	0.262	0.068644
27	560	18.458	18.735	0.277	0.076729
28	570	18.1515	18.475	0.3235	0.104652
29	580	18.356	18.233	-0.123	0.015129
30	590	16.824	18.009	1.185	1.404225

$$\varphi = 9 * 10^{-5} l^2 - 0.1277l + 61.899$$

$$SSE = 3.239$$

$$MSE = 0.115$$

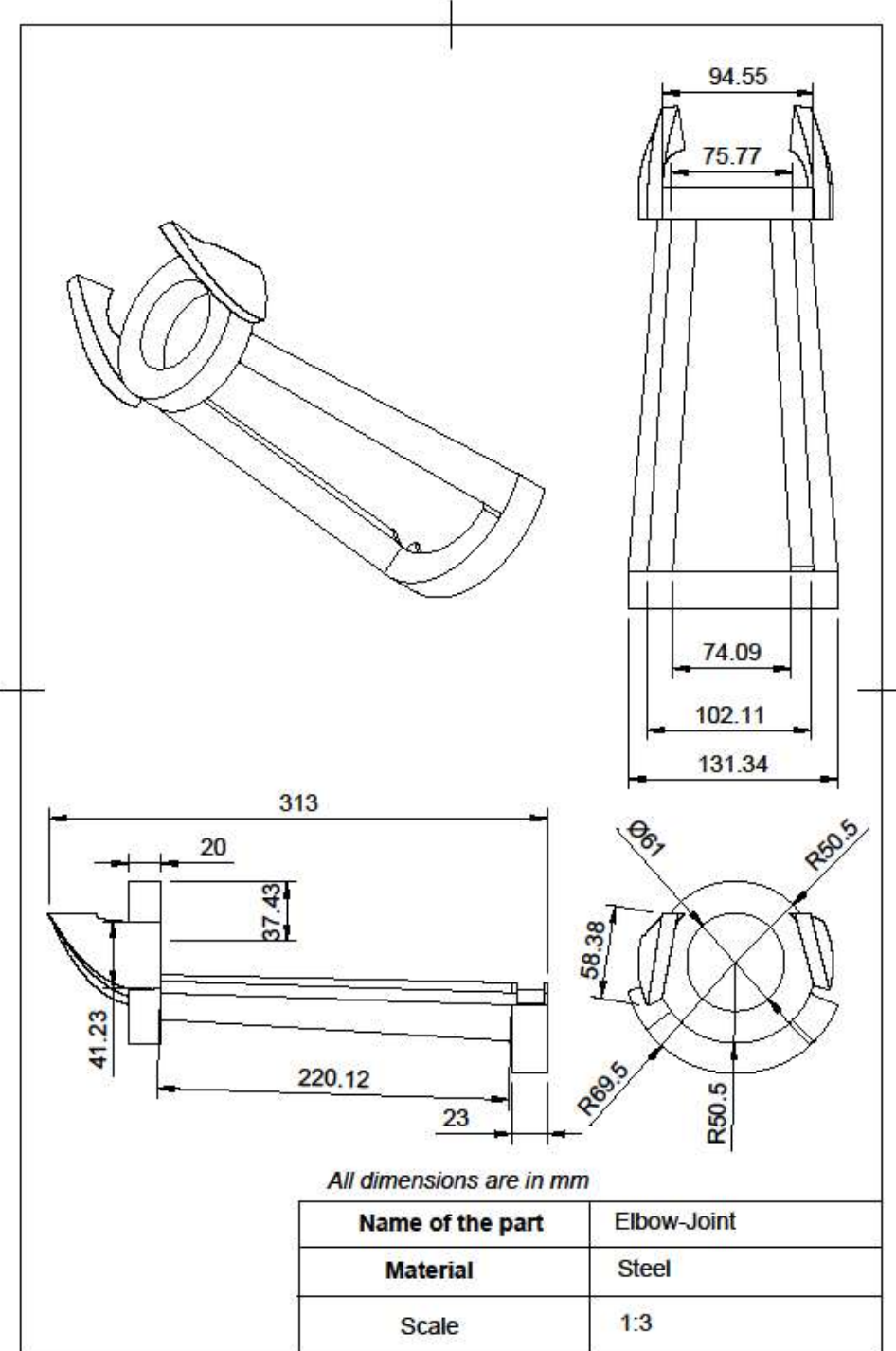
$$u(\varphi)_l = 0.340^\circ$$

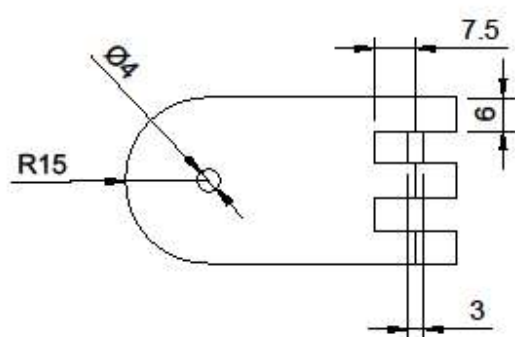
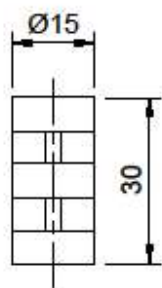
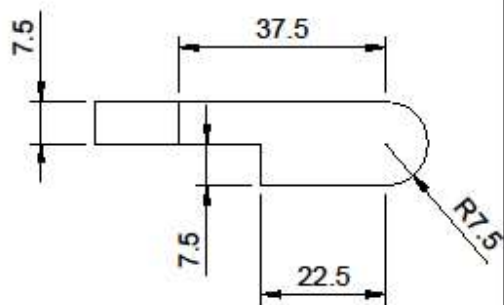
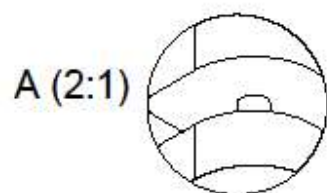
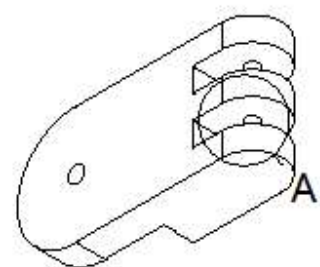
$$u(\varphi) = u(\varphi)_0 + u(\varphi)_l = 1.971$$

$$u(\varphi) = \pm 0.99^\circ$$

$$\emptyset = 9 \times 10^{-5} l^2 - 2 \times 10^{-7} \theta^2 + 0.1277l + 0.0062\theta + 42.295$$

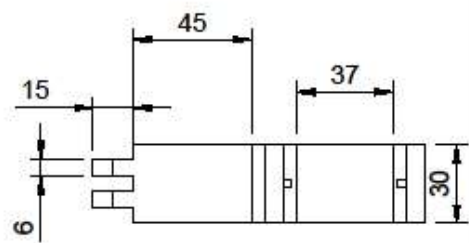
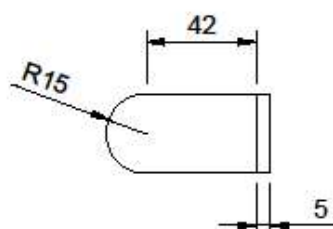
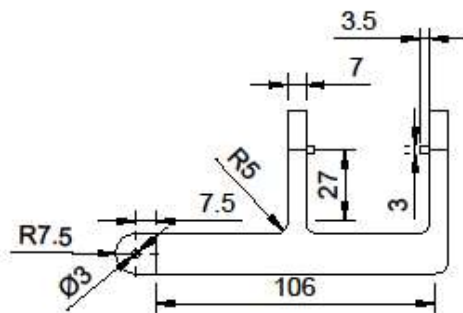
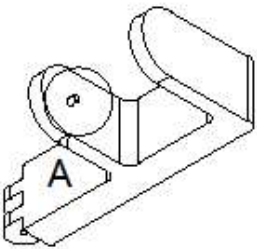
**APPENDIX III**  
**DRAWINGS OF CAD MODELS**





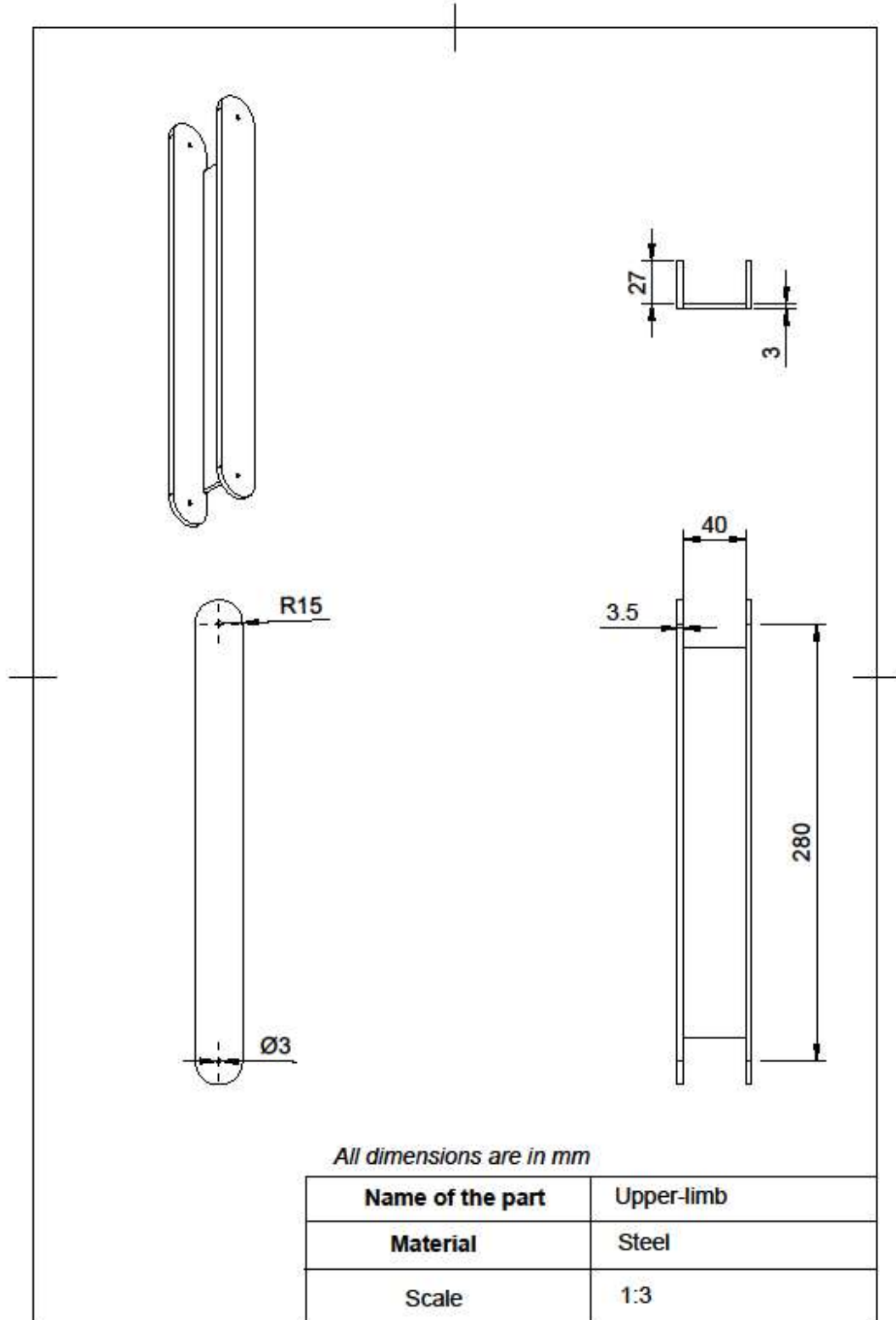
All dimensions are in mm

Name of the part	Part 1 Shoulder Complex
Material	Steel
Scale	1:1



All dimensions are in mm

Name of the part	Part 2 Shoulder Complex
Material	Steel
Scale	1:2



#### APPENDIX IV

## TECHNICAL DETAILS OF SIMULATWORK

### General

Contact Tolerance	0.1 mm
Remove Rigid Body Modes	No

### Mesh

Average Element Size (% of model size)	
Solids	7
Scale Mesh Size Per Part	No
Average Element Size (absolute value)	-
Element Order	Parabolic
Create Curved Mesh Elements	Yes
Max. Turn Angle on Curves (Deg.)	60
Max. Adjacent Mesh Size Ratio	1.5
Max. Aspect Ratio	10
Minimum Element Size (% of average size)	20

### Adaptive Mesh Refinement

Number of Refinement Steps	0
Results Convergence Tolerance (%)	20
Portion of Elements to Refine (%)	10
Results for Baseline Accuracy	Von Mises Stress

## APPENDIX V

### CODE FOR COMPUTER BASED IMPLEMENTATION

#### C1. MATLAB CODE FOR DH PARAMETER OF ARM

```

function dhrobot
a1 = 45; a2 =37.5; a3=83 ;a4=35;a5=280;a6=40;a8=220;
%L = Link ([Th d a alpha])
i=1;
x(:,:,1) = [0 0 0 0;0 0 0 0;0 0 0 0;0 0 0 0];
L(1)=Link([0 0 0 -pi/2]);
L(2)=Link([-pi/2 0 a2 -pi/2]);
L(3)=Link([-pi/2 a3 a4 -pi/2]);
L(4)=Link([pi/2 0 a5 0]);
L(5)=Link([-pi/2 0 a6+a8 0]);

Rob= SerialLink(L);
Rob.name='Exosuit'
Rob.plot([ 0 .872 -1.57 .349 .698]);
th1=0;
for th2= 0:0.1:1.57
for th3= 0.34: 0.1:1.39
for th4= 0.34: 0.1: 1.39
for th5= 1.22: .1: 1.57

%Rob.plot([th1 th2 th3 th4 th5 th6])
%x(:,:,i)=
Rob.fkine([th1 th2 th3 th4 th5])
i=i+1;
pause(0.15)
end
end
end
end

```

#### C2. MATLAB CODE FOR DEFINING EXOSUIT HAND

```

dhparams = [0.0375 -pi/2 0 -pi/2;
            0.042 -pi/2 0.083 -pi/2;
            0.28 0 0 pi/2;
            0.292 0 0.074269 -pi/2;]

robot = rigidBodyTree;
body1 = rigidBody('body1');
jnt1 = rigidBodyJoint('jnt1','revolute');

setFixedTransform(jnt1,dhparams(1,:),'dh');
body1.Joint = jnt1;

```

```

addBody(robot,body1,'base')
body2 = rigidBody('body2');
jnt2 = rigidBodyJoint('jnt2','revolute');
body3 = rigidBody('body3');
jnt3 = rigidBodyJoint('jnt3','revolute');
body4 = rigidBody('body4');
body5 = rigidBody('body5');
jnt5 = rigidBodyJoint('jnt5','revolute');

setFixedTransform(jnt2,dhparams(2,:),'dh');
setFixedTransform(jnt3,dhparams(3,:),'dh');
setFixedTransform(jnt5,dhparams(4,:),'dh');

body2.Joint = jnt2;
body3.Joint = jnt3;
body5.Joint = jnt5

addBody(robot,body2,'body1')
addBody(robot,body3,'body2')
addBody(robot,body4,'body3')
addBody(robot,body5,'body4')

showdetails(robot)
show(robot);

```

### C3. MATLAB CODE FOR SPECIFYING DYNAMIC PROPERTIES

```

robot = rigidBodyTree('DataFormat','row');

body1.Mass = 0.128597;
body1.CenterOfMass = [0.076369 .244844 .323843];
body1.Inertia = [1.208E-5 3.863E-5 3.076E-5 81.18E-9 521.08E-9 -
2911.226E-9];

body2.Mass = .557959;
body2.CenterOfMass = [.16324 0.239208 0.32142];
body2.Inertia = [1.638E-4 7.011E-4 7.831E-4 -2308.657E-9 1.728E-5
8.279E-5];

body3.Mass = 0.735587;
body3.CenterOfMass = [.180238 0.209039 0.18083];

```

```

body3.Inertia = [5.125E-3 5.329E-3 3.405E-4 -1.057E-4 -1.324E-4 -
516.592E-9];

body4.Mass = 1.274472;
body4.CenterOfMass = [102.963e-3 .133757 0.03627];
body4.Inertia = [1.684e-3 5.809e-3 4.745e-3 2.544e-4 4.097e-5 -
4.991e-4];

body5.Mass = 2.722225;
body5.CenterOfMass = [0.055706 -0.028736 -0.006563];
body5.Inertia = [2.554e-2 5.929e-3 2.618e-2 -1.357e-3 2.012e-3
2.085e-3];

```

#### C4. MATLAB CODE FOR DYNAMIC ANALYSIS

```

robot = rigidBodyTree('DataFormat','row');
jointVel = [% joint velocity values ]
jointAccel = [% joint acceleration values ]

% Matlab code for Computing joint torques for static joint
configuration

load exampleRobots.mat lbr
lbr.DataFormat = 'row';
lbr.Gravity = [0 0 -9.81];
q = randomConfiguration(lbr);
tau = inverseDynamics(lbr,q);

% Matlab code for computing Joint torques to counter external
force:

load exampleRobots.mat lbr
lbr.DataFormat = 'row';
lbr.Gravity = [0 0 -9.81];
q = randomConfiguration(lbr);
fext1 = externalForce(lbr,'tool0',[0 0 0.0 500 0 0],q);
tau = inverseDynamics(lbr,q,[],[],fext1);

% Matlab code for computing Forward dynamics due to external
force on the body:

load exampleRobots.mat lbr
lbr.DataFormat = 'row';
lbr.Gravity = [0 0 -9.81];
q = randomConfiguration(lbr);
wrench = [0 0 0.0 500 0 0];
fext = externalForce(lbr,'tool0',wrench,q);
qddot = forwardDynamics(lbr,q,[],[],fext);

```

## C5. ARDUINO CODE FOR PRESSURE SENSING

```
void loop() {
    int sensorValue= analogRead(A5);
    int voltage = sensorValue;
    Serial.println(voltage);
    delay(500);
}

void compressor(){
if (compressorCommand == true){
//convert the output to PSI to read the pressure of air tank
airTankPressure = (analogRead(airTankPressureSensor)*0.9)-Offset;
if (airTankPressure < TopPre){
digitalWrite(compressorPin, ON);
}
else if (airTankPressure >LowPre){
digitalWrite(compressorPin, OFF);
}
}
else if (compressorCommand == false){
digitalWrite(compressorPin, OFF);
}
}

void pressureSensor(){
//Measure air tank pressre and convert to PSI from datasheet formula of
MPX5010s
Serial.print("Air tank (PSI) = \t");
airTankPressure = (analogRead(airTankPressureSensor)*cvert;
Serial.print(airTankPressure);
Serial.print("\t");
}
```

```

//Measure muscle pressre and convert to PSI from datasheet formula of
MPX5010

Serial.print("Muscle (PSI) =\t");
musclePressure = (analogRead(airTankPressureSensor)*cvert;
Serial.print(musclePressure);
Serial.print("\t");
}

```

## C6. ARDUINO CODE FOR MUSCLE CONTROL

```

void startMotion(){

if (loadStart == true){

if(exomove == false){

p_millis = millis();

workcount = 0;

deadSwitch = false; }

exomove= true;

}

else if (loadStart == false){

exomove = false; }

//muscles have to be vented before use to remove previous load lag

digitalWrite(sValve_2, ON);

digitalWrite(mValve_2, ON);

diff=mills()-p_mills;

Serial.print(diff);

Serial.print("\t");

delay(1000);

digitalWrite(sValve_1, OFF);

digitalWrite(mValve_1, OFF); }

//decision for preassurization is checked

```

```

void motionCtrl(){

if (startMotion){

if (EMGIn>EMGTh && EMGIn<EMGH && diff>workcount +100 &&
diff<workcount+2000) {

digitalWrite(mValve_1, ON); // PIN to muscle
digitalWrite(sValve_1, ON); // PIN to valve
pcontrol=analogRead(A7);

}

//Muscle control

if (pcontrol>indcPressure&& pcontrol<maxPre && EMGIn>EMGTh&&
EMGIn>=EMGMax&& workcount<3200 ){

digitalWrite(mValve_1, ON);
digitalWrite(sValve_1, ON);
//Serial.println(diff);
Serial.print("Inflating ");
}

//Hold the muscle inflation

else if ( pcontrol>indcPressure&& pcontrol<maxPre&& EMGIn>EMGTh&& &&
workcount<4500{

digitalWrite(sValve_1, OFF);
digitalWrite(mValve_1, OFF);
Serial.print("Holding ");
}

// Release after work

else if (pcontrol<indcPressure && EMGIn==EMGTh){

Serial.print("Ready to deflate");
digitalWrite(mValve_2, ON);
digitalWrite(sValve_2, ON);
delay(2000);

Serial.print("Deflation Complete");
}
}
}

```

```
}

// Deadmans switch inclusion

if (deadSwitch && diff > 7000 +workcount){

workcount=workcount+10000;//force shoot counter overboard to halt
function

digitalWrite(mValve_2, ON);

digitalWrite(sValve_2, ON);

Serial.print("Valves open. Deflate complete. Suit Stopped ");

}

}
```